Characterizing Dual Transmission of the Middle Ear

Esther Sule

Thesis submitted to the Faculty of Graduate Studies in Partial Fulfillment of the Requirements for the Degree of Master of Science

Graduate Program in Physics and Astronomy

York University

Toronto, Ontario

January 2026

Abstract

The tympanic membrane (TM) is a component of the middle ear that provides a forward pathway for external sound energy to efficiently propagate to the inner ear. It is well established that the sensory cells of the inner ear also actively generate force that improves the ear's ability to encode sound. As a result, inner ears can create sound in the absence of external stimuli, known as spontaneous otoacoustic emissions (SOAE). These emissions leak back out through the middle ear in the reverse direction. We measured lizards' TM motions using a sensitive laser Doppler vibrometer and report spontaneous TM motion with displacements as small as several picometers, along with their relationship to SOAE measured simultaneously from the contralateral ear. Further, we measured motions induced by external sounds and computed the associated transfer function, as well as mapped out how these motions vary across the surface of the TM.

Acknowledgments

My utmost gratitude goes to God Almighty for seeing me through this journey. I sincerely thank my supervisor and mentor, Prof. Christopher Bergevin, for his outstanding support from the day I first reached out to express my interest in joining his lab to the completion of this work. His encouragement, valuable inputs, and guidance, especially during challenging moments, were instrumental to the milestones I achieved.

I am deeply grateful to my husband, Mr. Victor Sule, for his unwavering support and the many sacrifices he made to help me complete my master's degree. Many thanks to my mentors, Dr. Ilemona Omeje and Dr. Okeme Ilemona, for their encouragement and support since the days of my undergraduate studies till present. I appreciate the members of the Sensory Biophysics Lab, past and present (Rebecca E. Whiley, Olha Fedork, Rachel Laitman, and others), for their contributions during lab discussions and for creating a supportive research environment.

I also sincerely thank Prof. Natasha Mhatre for her valuable input and contributions throughout my research. I am grateful to my supervisory committee, Prof. Christopher Bergevin, Prof. Gloria Orchard, and Prof. Taylor Cleworth, for their guidance and feedback. Finally, I thank my children, parents, siblings, and in-laws for their love, patience, and support.

Table of Contents

List of Abbreviations

TM	Tympanic Membrane
OAEs	Otoacoustic Emissions
SOAE	Spontaneous Otoacoustic Emissions
SO	Spontaneous Oscillations
LDV	Laser Doppler Vibrometer
sLDV	Scanning Laser Doppler Vibrometer
dB	Decibel
SPL	Sound Pressure Level
MET	Mechanoelectrical Transduction
BM	Basilar Membrane
IAC	Interaural Cavity
FFT	Fast Fourier Transform
SNR	Signal-to-Noise ratio

List of Figures

Chapter 1

Introduction

1.1 Background

The ear is a complex biomechanical system that plays a crucial role in the detection of vibrations for hearing. In mammals, such as humans, the auditory periphery is divided into the outer, middle, and inner ear. The pinna and the ear canal make up the outer ear. The role of the outer ear is to collect sound waves from the external environment and direct them to the tympanic membrane (TM), or eardrum. The middle ear consists of the TM and the ossicular chain formed by the malleus, incus, and stapes (known as the three small bones). The stapes ends at the footplate, which rests on the oval window, the opening leading to the inner ear. When sound waves from the outer ear reach the TM, they are transformed into mechanical vibrations (Gentil et al., 2005).

The inner ear is made up of the vestibular system, which maintains balance, and the cochlea, which functions in sound detection. The cochlea is a spiral, fluid-filled structure lined with sensory cells called "hair cells" given their stereocilia (i.e, hair-like) projections (Manley, 1990). Because the cochlea is fluid-filled, higher pressures are required to drive fluid motion than to drive motion in air. Without a coupling mechanism, most of the incoming sound energy would be reflected at the air–fluid boundary.

The middle ear functions as an impedance matcher in the transmission of airborne sound to the fluid-filled inner ear. Acoustic impedance Z is a measure of opposition to sound motion and can be written as the ratio of pressure p to volume velocity U, $Z = \frac{p}{U}$. Because inner ear fluids have a much higher impedance than air, most sound would reflect at the boundary without a matching mechanism. The middle ear reduces this mismatch and therefore improves the efficiency of sound-energy transfer into the cochlea (Werner & Wever, 1972; Manley, 1990). The primary mechanism underlying this impedance matching is achieved through the difference in the effective areas of the eardrum and the stapes footplate and, to a lesser extent, the lever action of the ossicles (Wever & Wener, 1972).

Once sound energy is coupled into the cochlea, it is converted into a traveling wave and then into neural signals by the sensory epithelium. The basilar membrane (BM) is a flexible structure that runs along the length of the cochlea and supports the organ of corti (the receptor organ for hearing), which contains the hair cells. Vibration of the stapes footplate sets the cochlear fluids in motion and produces a traveling wave along the BM. The motion of the BM deflects the stereocilia bundles, and this bundle deflection opens mechanoelectrical transduction (MET) channels, producing a MET current that depolarizes the hair-cell membrane. Depolarization triggers neurotransmitter release at the hair-cell synapse and excites auditory-nerve fibres, transmitting sound information to the brain for processing (Natarajan et al., 2023).

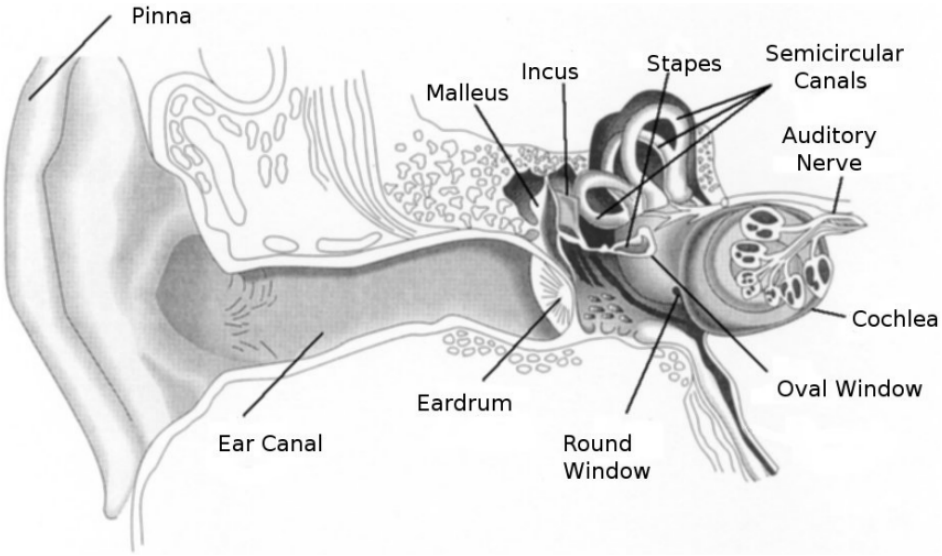

Figure 1.1: Schematics of the anatomy of the human ear (not to scale), adapted from Araujo et al., 2005. Typical adult dimensions for scale reference: the external ear is approximately 62.3 mm in length (Japatti et al., 2018), the TM has an area of approximately 55–85 mm^2, the malleus measures about 8–9 mm in length, the incus is typically 5–7 mm, and the stapes is approximately 3.25 mm in height with a footplate length of about 1.4 mm (Mansour et al., 2016). The cochlea has outer dimensions of approximately 10 mm $\times$ 8 mm $\times$ 4 mm (Kjer et al., 2016).

The inner ear exhibits an active process, termed cochlear amplification. In this process, sensory hair cells actively generate force using metabolic energy to boost low-level sounds and sharpen frequency selectivity. Because this active mechanism is energy-dependent, it introduces nonlinear behavior into cochlear mechanics (Dallos, 2008; Hudspeth, 2014). As a byproduct of this process, some acoustic energy can exit the inner ear, travel backward through the middle ear, and induce oscillations of the tympanic membrane, producing sounds called otoacoustic emissions (OAEs) (Kemp, 1979). OAEs can be measured noninvasively in the ear canal using a sensitive low-noise microphone. They are commonly classified as either evoked or spontaneous (Kemp, 1986). For the evoked otoacoustic emission (eOAEs), external stimuli, like tones or clicks, are presented first into the ear before OAEs are generated in response. In contrast, spontaneous otoacoustic emissions (SOAE) arise without any external acoustic stimulation. Previous studies have proposed that SOAEs arise from the activity

of groups of self-oscillating hair cells that interact in a noisy system (Gelfand et al., 2010; Vilfan and Duke, 2008). These emissions represent the combined behavior of the coupled hair cells in a given ear.

While the broader aim of this research is towards understanding the mechanisms underlying the generation and subsequent emission of SOAEs, which remain not fully understood, this thesis focuses on investigating the bidirectional transmission of sound energy at the level of the middle ear with a specific focus on the TM.

The middle ear plays dual roles in sound transmission: it transmits environmental sound to the inner ear, and it also transmits acoustic energy generated within the inner ear back to the ear canal, where it can be detected as OAEs (Dong & Olson, 2006). TM plays a vital role in the transduction process in both directions. Thus, our goal is to better characterize how both externally evoked sounds and internally generated SOAEs drive TM vibrations.

Otoacoustic emissions (OAEs) were first discovered in humans (Kemp, 1978) and have been studied extensively because of their clinical utility for newborn hearing screening. However, active inner-ear processes and OAEs are not unique to mammals; they are also observed in non-mammalian tetrapods (e.g., lizards and frogs) (Manley, 2000; Bergevin et al., 2008). Significant structural differences exist between mammalian and non-mammalian ears. It is therefore useful to provide an overview of non-mammalian ear anatomy. Here, we describe the lizard ear as a representative example.

1.2 Lizard Ears

Lizards lack a well-developed outer ear structure due to the absence of pinnae and a noticeable external ear canal, unlike mammals. In gecko species, for instance, the semi-transparent TM is oval-shaped, protrudes slightly outward, and lies only about 1–2 mm beneath the skin surface (Wever, 1978).

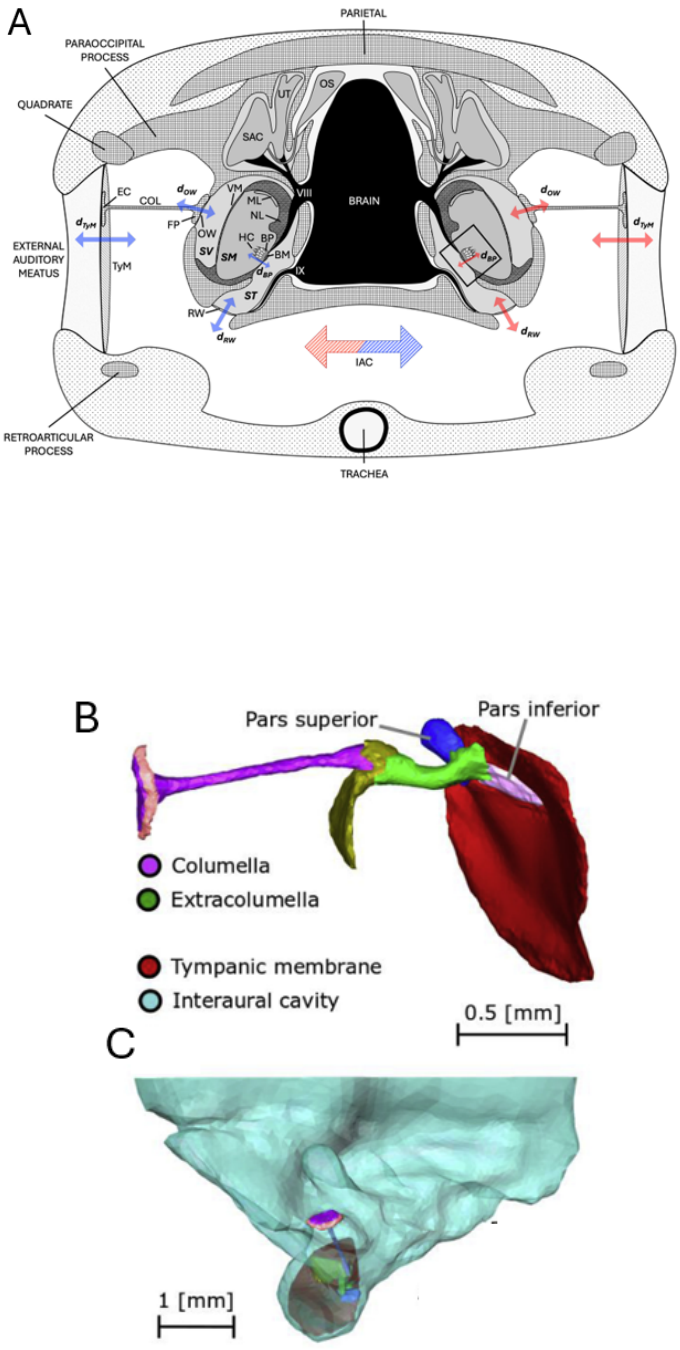

Figure 1.2: **(A)** Schematic of the cross-section of a lizard head showing the external auditory meatus (external ear canal), inner ear, and the interaural cavity (IAC) linking the two ears. Arrows indicate the motion pathways that transmit acoustic energy in the left (blue) and right (red) ears, while the bicolored striped arrow indicates interaural coupling through the IAC (adapted from Fig. 7, Whiley et al., 2025). **(B–C)** Micro-CT–based 3D reconstruction of middle-ear structures (adapted from Livens et al., 2019).

The middle ear contains a single ossicle known as the columella, which extends into a cartilaginous extracolumella with additional attached processes. The pars superior and pars inferior together form a continuous rod that runs from the dorsal edge of the TM toward a point near its center (Wever 1972). The columella is located in an air-filled middle ear cavity. This cavity opens into and connects to the oral cavity; together, they form an interaural cavity (IAC) that acoustically links the left and right ears (Christensen-Dalsgaard, 2005). The bony columella is coupled to the TM by soft connective tissues and terminates in a footplate that rests on the oval window, similar to the mammalian stapes. When sound reaches one ear, it drives TM vibration and generates pressure fluctuations within the middle-ear cavity. These pressure waves can propagate through the IAC to the opposite side of the head and act on the internal surface of the contralateral (opposite) TM. As a result, each TM is driven by sound coming both from the external environment and through the internal pathway within the head. This mechanical coupling creates a means by which the two ears act as a pressure-gradient receiver that provides directional cues for binaural sound localization (Christensen-Dalsgaard & Manley, 2005). The inner ear of lizards is not coiled, as found in mammals, but contains a straight cochlea, known as the cochlear duct. Inside the cochlear duct lies the organ of Corti, called the basilar papilla, a structure where the hair cells are located. These hair cells are arranged in a tonotopic manner along the length of the duct. In most arrangements, the basal end responds to low frequency sounds while the apical end responds to high frequencies (Manley et al.,1999). The size of the basilar papilla and the number of hair cells are different between species of lizards. For example, in anole lizards, the basilar papilla is around 0.4 mm long and 0.1 mm wide and contains about 150 hair cells (Miller, 1981; Negandhi et al., 2018). In contrast, the basilar papillae in gecko lizards are about 2 mm long and between 0.05 and 0.13 mm wide and contain about 2,000 hair cells (Miller, 1973; Gelfand et al., 2010). Since each inner ear functions as an active self-oscillator, binaural coupling between the two ears may produce binaural synchronization. That is, the ears could synchronize because of their weak interaction via the IAC, causing the oscillators

of each inner ear to adjust their characteristic frequencies (Pikovsky et al., 2001). Despite differences in ear anatomy, hearing processes in mammals and lizards are the same.

1.3 Biomechanics of the TM

As mentioned earlier in section 1.1, the goal of this research is to better characterize how both externally evoked sounds and internally generated SOAEs drive TM vibrations. Although OAEs originate within the inner ear, detection in the external canal requires backward transmission through the middle ear ossicles, which induces displacement of the TM, where mechanical stimulation is transformed into sound pressure (OAE), which can be detected by a sensitive microphone probe. Previous studies have extensively examined the bidirectional transmission of sound in mammals (Dong and Olson, 2006; Cheng et al., 2011, 2019). In studies of forward sound transmission in humans, the TM moves approximately in-phase across most of its surface at low frequencies (0.5–10 kHz), with only small local phase delays near regions of maximal displacement. At higher frequencies (4–8 kHz), the vibration pattern becomes more complex, with multiple displacement maxima and a mixture of in-phase and out-of-phase regions (Cheng et al., 2009). The TM also responds broadly to external sound stimuli from the environment, with an increase in the pressure transmitted to the inner ear and attenuation in the backward transmission (Megan et al. 1972, Puria 2003). Similarly, studies on the forward transmission of sound in lizards also reveal that at low frequencies, the eardrum moves in phase, whereas at higher frequencies it shows greater phase variation (Manley, 1972). Direct studies of TM vibration during backward transmission in lizards are limited. Bergevin et al. (2018) provided the first direct mechanical evidence by measuring picometer-scale TM vibration driven by internal forces in one ear while simultaneously recording SOAEs from the contralateral ear. Their results highlighted both similarities and differences between the spectral features of TM vibration and the simultaneously recorded SOAEs (see section 1.3), motivating further work to characterize TM mechanics across both

forward and backward transmission pathways.

1.4 Research Motivation

Our rationale for studying OAEs is to better understand the mechanisms that generate them. Although our ultimate interest is in human hearing, direct investigation in humans is quite challenging. One major reason is that the inner ear is encased within the bony skull, which makes it difficult to access without damaging delicate sensory structures. Therefore, we conducted experiments in live lizards, which are known to emit robust OAEs (Manley and Kemp, 2008) and have a relatively simpler auditory system that nonetheless functions well for hearing. In addition, their accessible external ear makes it easier to measure TM motion. Bergevin et al. (2018) provided the direct mechanical evidence of active processes in live lizards at the level of the tympanic membrane. Using laser Doppler vibrometry (LDV), a noninvasive measurement tool (see chapter 2, section 2.1), they measured TM vibrations driven by active forces from the inner ear in the absence of external sound and simultaneously recorded SOAEs from the opposite ear (contralateral ear) in a green anole lizard.

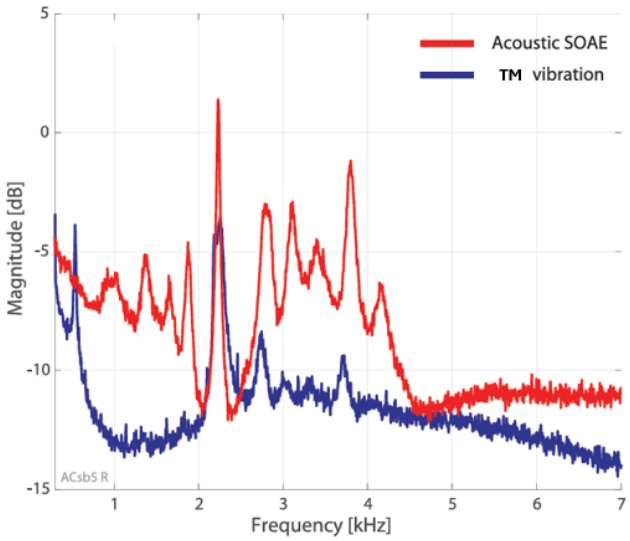

Figure 1.3: Green anole TM vibration spectrum (blue) and simultaneously recorded acoustic SOAE spectrum from the contralateral ear (red) in the same animal. Adapted from Bergevin et al. (2018).

As shown in Figure 1.3, prominent spectral peaks rising above the noise floor (i.e., the minimum detectable level set by the measurement system) indicate frequencies at which inner-ear activity is concentrated. Bergevin et al., (2018) reported displacement amplitudes of approximately 60 pm at 3.9 kHz for a strong spectral peak in the green anole. By comparing TM vibration from one ear with simultaneously recorded SOAEs from the contralateral (opposite) ear, they found some correspondence in spectral peak locations; however, some SOAE peaks do not have corresponding TM peaks. They suggested that the mismatch is due to the discordant nature of TM vibrations, in which different TM locations can exhibit distinct spectral peaks. These findings motivate the key questions that guide the present study and form the basis of our hypotheses.

1.5 Questions Guiding the Current Research

The following are the questions guiding our present study.

- Do non-simultaneously measured spontaneous vibrations from the right and left TM in the same lizard exhibit similar spectral peaks?
- Why do some distinct spectral peaks in the SOAEs recorded from one ear lack corresponding SO peaks at a single measurement point on the opposite TM in the same lizard?
- Do spontaneous oscillation peaks of the TM in one ear exhibit phase coherence with simultaneously measured contralateral SOAEs?
- Do vibrations across the visible surface of the TM, as induced by external sound, exhibit nonlinearity to sound pressure levels (SPLs)?

1.6 Hypotheses

- Because lizards' right and left ears are interaurally connected, both TMs will exhibit similar spectral peaks in their spontaneous oscillations.
- Spontaneous TM spectral peaks in one ear will be phase coherent with simultaneously recorded contralateral SOAEs.
- Sound-evoked TM motion will exhibit nonlinear mechanical behaviour to varying SPLs since OAEs reveal nonlinear acoustic responses in the ear canal.

Chapter 2

MATERIALS AND METHODS

2.1 EXPERIMENTAL SETUP

2.1.1 Scanning Laser Doppler Vibrometry System

The scanning laser Doppler vibrometry system (sLDV) is a non-invasive and highly sensitive instrument used to directly measure the velocity of vibrating surfaces. Through the use of an interferometer, the laser beam is divided into a reference beam and a measurement beam. The measurement beam is directed onto the vibrating surface, and the reflected light is recombined with the internal reference beam. The sLDV is based on the principle of the doppler effect to determine surface velocity through the comparison between the frequency of the outgoing laser light with that of the reflected light. The frequency of the reflected light is modulated by the velocity of the vibrating surface, and the interference between the reference and reflected beams generates a beat frequency. The vibrometer decodes this beat frequency to determine the instantaneous velocity of the vibrating surface (Gatzwiller et al., 2002). In addition, although the sLDV directly measures velocity, displacement information can be derived through numerical integration of the velocity signal. We employed sLDV (Polytec, PSV-500) in full-field mode to measure the vibration of the visible surface of the TM. The system can also be operated in single-point mode, which we used in selected cases

to enable direct comparison with previous single-point measurements (e.g., Bergevin et al., 2018).

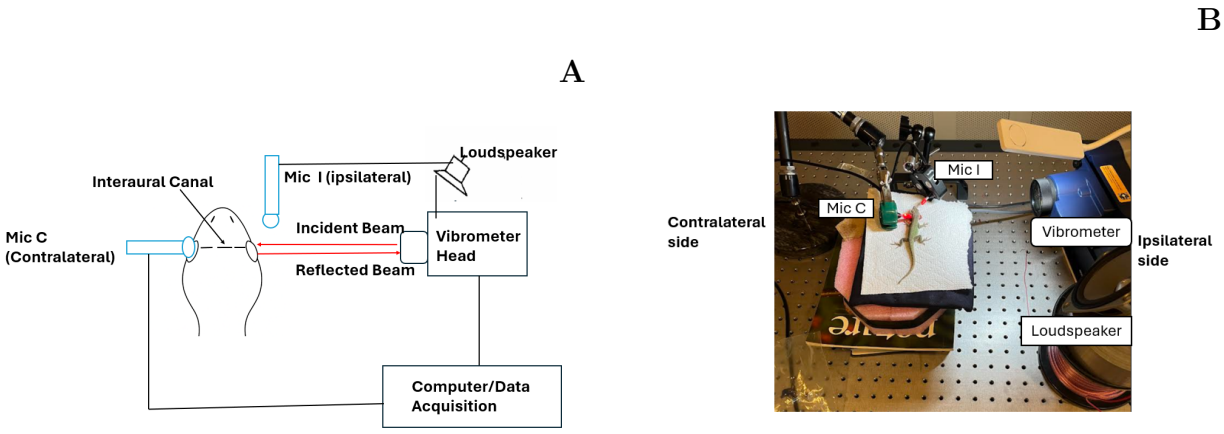

Figure 2.1: **(A)** Schematic of the experimental setup for measuring tympanic membrane (TM) vibration under sound-evoked (SE) and spontaneous (SO) conditions. The laser beam from the vibrometer is directed onto the TM to measure its surface velocity. Spontaneous TM motion is recorded without external acoustic stimulation, with Mic C (ER10C-3) coupled to the contralateral ear to capture SOAEs. For sound-evoked measurements, a loudspeaker delivers the stimulus while Mic I (ER10C-2), placed ipsilaterally, records the incident sound pressure. **(B)** Photograph of the corresponding experimental setup.

The lizards were placed on top of a microfluidic device to raise it slightly relative to the laser beam to ensure a proper and clear focus of the laser beam on the TM. In laser Doppler vibrometry, sufficient reflectivity of the vibrating surface is required to obtain high signal-to-noise measurements. Because the TM was reflective, we did not place additional reflective material. We focused the laser beam perpendicular onto predefined measurement points arranged into a grid on the visible surface of the TM in a two-dimensional space. with an average point-to-point spacing of approximately 0.22 mm (see Appendix A.1). During the scan, the laser beam moves from one measurement point to another, recording the velocity at each location. Scanning across multiple points on the TM surface provides a spatially resolved vibration pattern over the entire TM's surface. As noted prior, we focused on the measurement of two distinct types of TM motions: spontaneous and sound-evoked vibrations. The next subsections define the sound-evoked and simultaneous measurement

conditions used in this study.

2.1.1.1 Sound Evoked TM Measurement

This refers to TM motion measured in the forward transmission pathway, where the TM is stimulated by an external acoustic source, such as a loudspeaker.

2.1.1.2 Spontaneous TM Measurement

This refers to the backward transmission pathway where TM motion is driven by the internally generated active forces of the inner ear. It is measured in a quiet environment, in the absence of any external acoustic stimulation. In this study, we refer to this motion as spontaneous oscillation (SO), which represents the TM displacement that arises without external acoustic stimulation. Spontaneous oscillations (SO) appear as narrowband spectral peaks that rise above the experimental noise floor at specific frequencies. These peak frequencies indicate where spontaneous inner ear activity or spectral energy is strong in the spectrum. It is important to note that the spontaneous motion of the TM gives rise to SOAEs that can be recorded in the ear canal. In this study, we measured both sound-evoked and spontaneous oscillations using the sLDV measurement system.

2.2 Animals Preparations

This study received ethics approval (protocol 2016-21 R2) from the Animal Care Committee (ACC) under the Office of Research Ethics (ORE) at York University, Canada. We conducted experiments on two species of healthy lizards; these consisted of six adult male green anoles (Anolis carolinensis), weighing between 3.3 and 8.1 g, and four leopard geckos (albino morph; Eublepharis macularius), comprising one male and three females, weighing between 24.3 and 50.5 g. Before the measurements, all the animals were lightly anaesthetized via intraperitoneal or subcutaneous injections. Anoles received Euthanyl (32 to 34 mg/kg, de-

pending on body weight), and geckos received Alfaxalone (30 mg/kg). After the induction, we placed the anaesthetized lizards in an acoustic isolation booth to reduce external noise interference during our measurement. We also minimized the fluctuation in body temperature during the measurement by placing each lizard on a regulated heating pad set to 30°C. This ensured the lizard remained physiologically stable throughout the experiment. Following the measurements, all animals fully recovered from anesthesia and were returned to their housing.

2.2.1 Measurement of TM Surface Motion

We measured the spontaneous oscillation of the visible surface of the TM in the absence of external acoustic stimulation. To do this, we focused the laser beam on the ipsilateral TM (the ear directly facing the laser), while on the contralateral side, a sensitive microphone probe (Etymotic ER-10C) was directly coupled and sealed with grease to the external auditory meatus (external ear canal). This arrangement enabled the simultaneous measurement of spontaneous oscillations of the TM in one ear and the recording of SOAEs from the contralateral ear.

For the sound-evoked measurements, the TM was stimulated with a chirp frequency stimulus ranging from 0.5 to 10 kHz at varying sound pressure levels across 7 to 69 dB SPL, with the contralateral ear blocked by coupling a microphone to the external auditory meatus. The rationale for choosing 0.5–10 kHz is not that it represents the exact hearing range of lizards. Rather, we selected a band that is broad enough to capture the frequency range over which the middle ear is expected to transmit useful vibration to the inner ear and to identify where the TM response begins to roll off. Ruggero & Temchin (2002) emphasize that audiogram bandwidth is not determined solely by outer or middle ear mechanics; instead, inner ear mechanics strongly contribute to both the low and high frequency limits. The sound pressure was kept constant during the 80 ms chirp. Each measurement was carried out in an open field, with acoustic stimulation delivered from a loudspeaker positioned close

to the animal. We placed a microphone probe (ER10C-2) about 1–1.5 cm from the edge of the TM surface to record the incident sound pressure.

For both spontaneous and sound-evoked measurements, data were acquired repeatedly at each scan point to enable averaging and thereby improve the signal-to-noise ratio (SNR). Two averaging approaches were used: temporal averaging and spectral averaging, which are discussed in sections 2.2.1.1 and 2.2.1.2, respectively.

2.2.1.1 Temporal Averaging

Temporal averaging involves averaging in the time domain across repeated recordings obtained under the same stimulus/condition. Because random noise varies between repeated acquisitions, it tends to cancel out, while the repeatable component of the response is reinforced. This improves the SNR, particularly when the response is time-locked and consistent across repetitions (see Appendix A.4 for temporal averaging and noise floor dynamics). Since our analysis is performed in the frequency domain, the temporally averaged waveform is subsequently transformed using the fast Fourier transform (FFT).

2.2.1.2 Spectral Averaging

The averaging is performed in the frequency domain by computing the spectrum using the FFT for each repeated recording and then averaging the resulting spectra. This reduces random fluctuations due to noise, giving a cleaner and more repeatable spectrum across frequency.

After data acquisition, we performed temporal averaging of the sound-evoked measurements. This approach is appropriate because the sound-evoked TM response is time-locked to the stimulus, so repeatable components add coherently while random noise tends to cancel. For spontaneous recordings (SO and SOAEs), there is no external timing reference, so averaging was performed in the frequency domain by computing spectra from repeated time segments and averaging the resulting spectral estimates. The raw data were saved in the

Polytec software as PSV files and exported for further analysis in Python.

2.3 Transfer Function

A transfer function is a frequency domain description that characterizes how a linear system transforms an input signal into an output signal, thereby characterizing the system's dynamic behaviour. In this study, we calculated the transfer function of the TM during forward transmission. The incident sound pressure, measured close to the TM with a microphone probe (ER-1OC), was taken as the input, while the vibration of the TM was the output. The transfer function was computed by taking the ratio of the Fourier transform of the TM response to the incident sound pressure across the entire frequency range, and we obtained both the magnitude and phase components of the transfer function. The magnitude quantifies the amplitude of TM motion per unit sound pressure at each frequency, while the phase describes the time of TM motion relative to the acoustic stimulus.

It is mathematically defined below as:

$$H(f) = \frac{V(f)}{P(f)}$$

$$H(f) = \textit{Transfer function at frequency } f$$

$$V(f) = \textit{Frequency domain Velocity of the TM vibration}$$

$$P(f) = \textit{Incident sound pressure in frequency domain}$$

Chapter 3

Investigating Spontaneous Oscillations of the Tympanic Membrane

Hypothesis 1: ***Because lizards' right and left ears are interaurally connected, both TMs will exhibit similar peaks in their spontaneous oscillations.***

As previously mentioned in Chapter 1, SOAEs reflect active processes in the inner ear. These emissions propagate backward through the middle ear via the ossicles, ultimately setting the TM into vibration. This bidirectional middle-ear transmission pathway means that the TM is not only a passive receiver of external sound but also an output interface through which active inner-ear processes can be expressed. In lizards, interaural coupling via the interaural cavity (IAC; chapter 1, section 1.2) means that TM motion in one ear may be influenced by pressures transmitted from the contralateral ear. Although this coupling is mainly considered in the context of passive sound localization, it also raises an important question: whether active inner-ear activity from both ears interacts through this shared interaural pathway. Specifically, whether spontaneous vibration patterns measured from the right and left TMs in the same lizard exhibit similar spectral characteristics.

Before addressing the guiding question and hypothesis of this chapter, we first characterized the spatial patterns of spontaneous oscillation of the TM using the sLDV measurement

system, extending the single-point TM measurements reported by Bergevin et al. (2018). In their study, they observed some correspondence in spectral peak locations between TM oscillations and contralaterally recorded SOAEs, although some SOAE peaks lacked corresponding TM spectral peaks. This present approach provided a full-field view of TM vibration and allowed us to examine the distribution of SO spectral peaks across its surface, as well as spatial variation in the noise floor, which may mask some SO spectral peaks at certain locations. Having established this approach, we next investigated whether the acoustic connection of the lizard's middle ears, through the interaural cavity, also manifests in the spontaneous SO peaks in the two tympanic membranes.

3.1 Result

3.1.1 Spatial Variations in TM Spontaneous Oscillations

To better characterize the spatial profile of spontaneous TM oscillations, we analyzed the vibration spectra across three anatomically defined regions: dorsal (upper portion of the TM, closer to the head), middle, and ventral (lower portion, closer to the jaw), as shown in Figure 3.1 (A). As expected, the spectral peak locations were consistent across regions, but the amplitudes varied substantially. Across the examinations we conducted on three anoles, we consistently observed that the dorsal region exhibited few or no distinct peaks, while the middle region showed some peaks of moderate amplitude. In contrast, the ventral region consistently showed more pronounced peaks. Figure 3.1(B) is representative data, which was typical of the other individuals scanned.

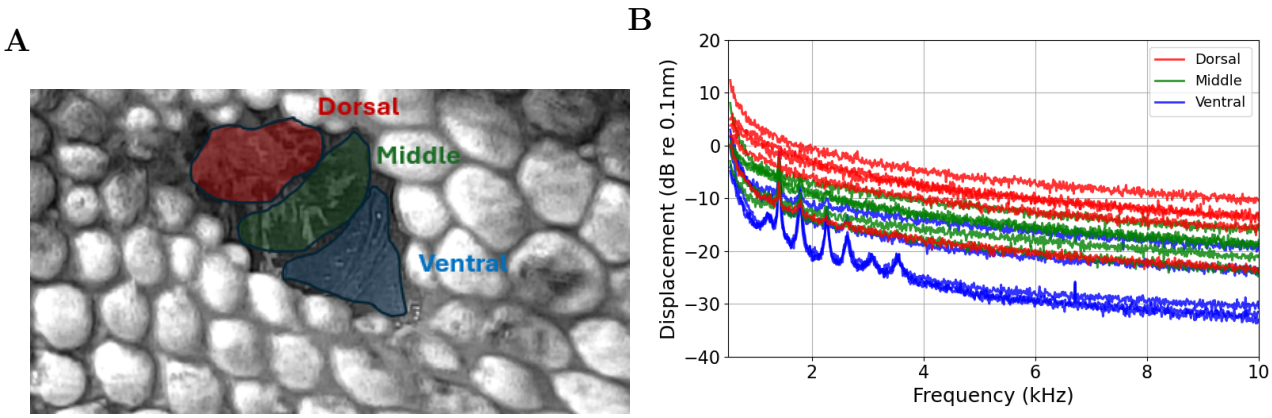

Figure 3.1: (A) Anatomical distinction of the visible surface of the anole TM into dorsal (red), middle (green), and ventral (blue) regions. (B) Spontaneous TM oscillation spectra (displacement re 0.13nm) from representative sLDV scan points in the dorsal, middle, and ventral regions, illustrating spatial variability in SO peaks across the TM surface.

We attribute the reduced peak visibility in the dorsal region to its higher local noise floor relative to the ventral and middle regions. This interpretation is supported by the observation that a spectral from the dorsal location (red curve) overlaps in amplitude with the ventral spectral (blue curves), which has a lower noise floor. Thus, it is likely that most SO peaks in the dorsal region were masked by an elevated noise floor, which we attribute to poor reflectivity at those measurement locations, rather than a lack of SO peaks. If the dorsal noise floor were reduced, we would expect to detect more prominent SO peaks, comparable to those consistently observed in the ventral region.

3.1.2 Noise Floor Variability on TM Surface

As suggested by the spectral analysis in Figure 3.1(B), the noise floor is not uniformly distributed on the TM surface. To investigate this further, we computed a spatial profile of the noise floor by quantifying the mean spectral amplitude in frequency bins corresponding to the valleys surrounding the tallest SO peak. This approach allowed us to isolate regions without SO peaks and estimate their baseline noise levels. From the same representative anole shown in Figure 3.1(B), we computed the mean values of the valleys surrounding the

tallest SO peak (1.14 kHz) across the visible TM surface and visualized them as a spatial heatmap shown in Figure 3.2.

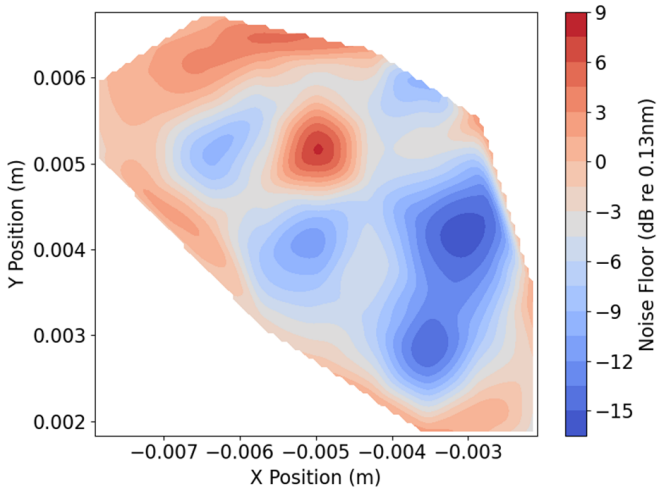

Figure 3.2: Spatial map distribution of the TM noise floor in a green anole lizard.

The blue regions correspond to a lower noise floor, while those shown in red correspond to elevated noise floor levels. In addition to the dorsal region with a higher noise floor, we also observed a localized noise floor elevation near the middle region of the TM. These spatial variations are consistent with our earlier observation that the dorsal region often lacked SO peaks, followed by moderate peaks in the middle region. We interpret this as evidence that an elevated local noise floor, likely due to reduced optical reflectivity of the TM surface, can mask low-amplitude SO spectral peaks. In contrast, ventral regions with a lower noise floor exhibited more clearly defined SO spectral peaks. Also, spatial heterogeneity in TM stiffness may contribute, with the ventral region vibrating more than the dorsal region (Han Young, 2018).

3.1.3 Signal-to-Noise Ratio (SNR) of Spontaneous TM Oscillation

We further investigated whether the regions with lower local noise floors observed in Figure 3.2 correspond to the regions where prominent SO peaks are exhibited. To test this, we computed a spatial SNR map of the TM spontaneous data. Here, the signal was defined as

the spectral magnitude at the tallest SO peak (1.41 kHz), and noise as the mean magnitude from the adjacent valley bins on either side of that peak (the same bins used in the noise floor analysis). SNR was then expressed in decibels as the ratio of signal to noise at each scan point. As shown in Figure 3.3, regions with high SNR (red) were localized primarily to the ventral TM, indicating that SO peaks were well above the baseline noise floor in this area. In contrast, the dorsal region of the TM has low SNR values (blue), consistent with our earlier observations that it often lacked visible SO peaks.

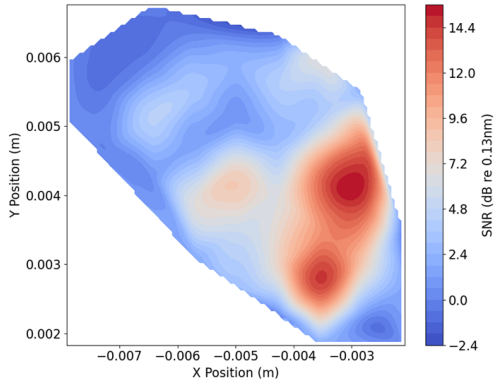

Figure 3.3: Spatial SNR of spontaneous TM oscillation (dB re 0.13 nm). At each scan point, SNR was computed as the ratio of the tallest SO peak to the mean of adjacent valley bins.

3.1.4 Spontaneous Oscillations in Right versus Left TM

To obtain these measurements, we used the same traditional setup described in the Materials and Methods (Chapter 2) for spontaneous measurements. In this setup, the laser beam was focused on the TM of one ear to measure SO, while the contralateral ear was closely coupled with a microphone probe to record SOAE. For this experiment, after measuring the SO from one ear, the lizard was carefully repositioned so that the other ear, previously used for SOAE recording, was now aligned for TM measurement, and vice versa. This procedure allowed us to obtain both SO and SOAE measurements from the right and left ears of the same animal, collected approximately two hours apart.

Figure 3.4 shows a representative example from a green anole. In this individual, the

right TM was measured first, followed by the left TM two hours later. The SO spectra from the right (blue) and left (red) TMs both exhibit multiple SO peaks across similar frequency regions. A small frequency shift was observed between the two spectra, with the left ear SO peaks shifted toward lower frequencies compared to the right ear SO peaks (blue). This shift caused a minor mismatch between the two spectra. Despite these differences, their overall peak patterns remained consistent.

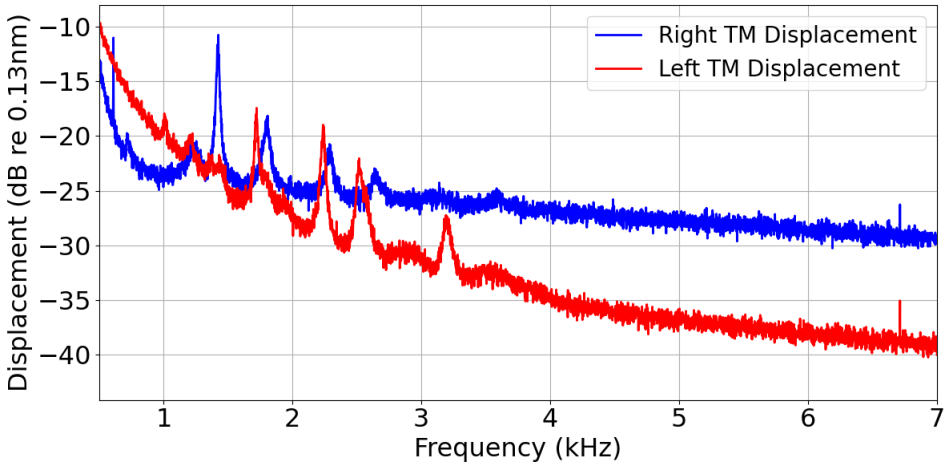

Figure 3.4: Comparison between right and left SO spectra recorded two hours apart in the same anole lizard.

3.2 Discussion

Our results provide new insights into the spontaneous motion of the lizard TM by extending previous single-point measurements (Bergevin et al., 2018) to spatially resolved full-field recordings. Using sLDV, we characterized how spontaneous oscillations vary across the visible surface of the TM and how differences in local noise floor levels influence the visibility of spectral peaks. These findings suggest that spatial heterogeneity in the noise floor is closely linked to the optical reflectivity of measurement locations, which directly affects the sensitivity of LDV measurements.

One limitation of this study is that we did not enhance the TM reflectivity by applying reflective material to the visible surface. We presume that doing so in future experiments

may help reveal additional spectral peaks currently masked by poor reflectivity. A second limitation is that we obtained full-field scans only in the anole, whereas measurements in the gecko TM were limited to single points. Full-field scans in the gecko would have provided a broader basis for species comparisons and enabled the examination of SO motion in a lizard with a larger TM. Thus, the absence of visible SO peaks in some regions does not necessarily indicate a lack of vibration; rather, these oscillations may be present but obscured by elevated local noise levels because of poor reflectivity on the TM surface.

Because lizards are ectothermic animals (their body temperature depends on the surrounding environment), the frequency shift observed in the spontaneous oscillations between the two ears, measured at different times in the same individual, is likely attributable to changes in body temperature. We did not continuously monitor the temperature while recording, but previous research has shown that SOAE frequencies change systematically with temperature. Warmer conditions cause the frequencies to go up, while cooler conditions cause them to go down (Manley, 2006). Since the spontaneous oscillation of the TM gives rise to spontaneous otoacoustic emissions, we reasonably infer that SOs are also temperature-sensitive; hence, the subtle frequency mismatches observed between the right and left TM measurements (Figure 3.4) reflect temperature-induced frequency shifts rather than measurement inconsistencies.

To further validate this, we compared the simultaneously recorded SOAEs from both ears of the same animal (see Appendix A.2). We observed minor spectral mismatches between corresponding SOAE peaks, consistent with temperature variations occurring between measurement sessions.

Chapter 4

Interaural Coupling and Binaural Synchrony

Hypothesis 2: ***Spontaneous TM oscillations in one ear will be phase coherent with the simultaneously recorded contralateral SOAEs.***

Phase coherence (ranging from 0 to 1) provides a quantitative measure of how consistently the phase of two signals aligns over time. A coherence value of 1 means the signals are perfectly in synchrony, while a value of 0 means they are completely independent. In auditory research, phase coherence is often used to evaluate how strongly different oscillatory sources are coupled. In lizards, SOAEs provide evidence for such coupling. Specifically, recent studies suggest that SOAEs recorded from one ear could derive energy from both ears through acoustic interactions in the interaural cavity (IAC). For example, Roongthumskul et al. (2019) simultaneously measured SOAEs from both ears in tokay geckos and reported that SOAE peaks appeared at similar frequencies in the two ears, and these matched peaks coincided with regions of high phase coherence (quantified as vector strength). These findings strongly support the existence of coupling between the ears. Bergevin et al. (2020) also reported evidence of IAC as a means of binaural synchronization by recording SOAEs directly from the oral cavity of the green anole. They reported that SOAEs recorded from the oral

cavity (which were presumed to represent contributions from both ears) showed striking similarities to those measured from either ear alone. These results raise the possibility that spontaneous oscillation of the TM could also exhibit this coupling when compared directly with contralateral SOAEs measured simultaneously. In this study, we investigated phase coherence between spontaneous TM oscillation in one ear and simultaneously recorded SOAEs from the contralateral ear. This approach allows us to examine whether TM vibration is synchronized with acoustic emissions from the contralateral ear.

4.1 Result

We examined the phase coherence between spontaneous oscillations of the TM and simultaneously recorded SOAEs from the contralateral ear in both the green anole and the leopard gecko. As shown in Figure 4.1 (A), the frequencies at which SO activity was present in the TM corresponded with the frequencies of SOAEs recorded from the contralateral ear. These matched frequencies also coincided with spectral peaks in the phase coherence spectrum. For instance, in the representative anole shown in Figure 4.1 (A&B), we observed that the bigger SO peak at 1.14 kHz corresponds to a high phase coherence value of approximately 0.8, and a smaller SO peak at 3.13 kHz exhibited a lower coherence value (0.2).

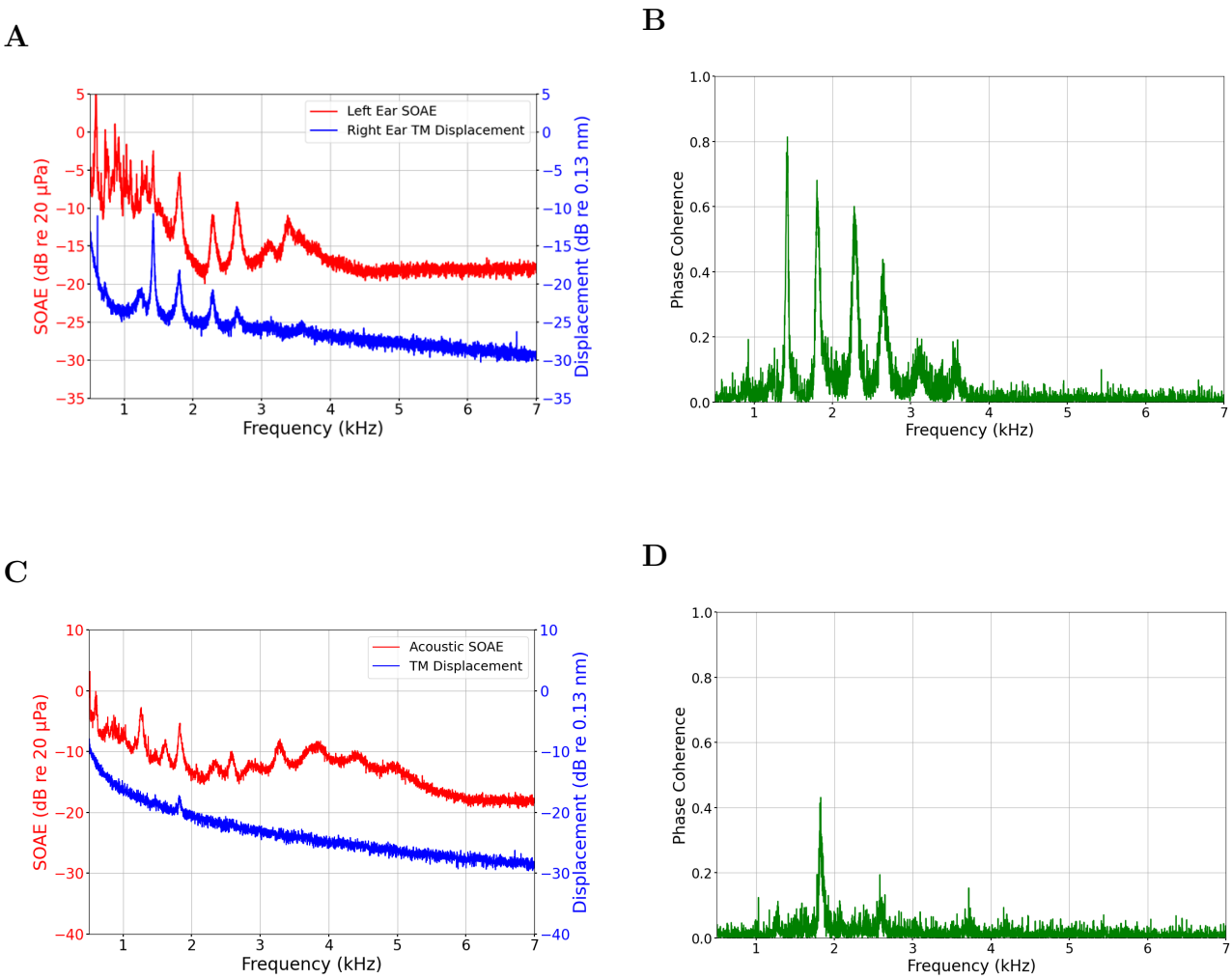

Figure 4.1: (A) Spontaneous oscillation of the right TM (blue) in an anole (subject 1) recorded simultaneously with SOAE (red) from the left ear. (B) Corresponding phase coherence between TM spontaneous oscillations and contralateral SOAEs in the same animal. Peaks in coherence (ranging from 0 to 1) indicate strong binaural synchrony, consistent with binaural coupling between the ears. (C) Spontaneous TM oscillation (blue) and contralateral SOAEs (red) for a second anole (subject 2). (D) Phase coherence for subject 2 showing fewer and weaker spectral peaks, suggesting reduced binaural synchrony compared to subject 1.

In contrast, leopard geckos showed no measurable SO peak in any of the four individuals examined. In two of the geckos, the SOAEs recorded from the contralateral ear were weak emissions. As illustrated in Figure 4.2 (A&B), a representative gecko had no distinct SO peaks in the TM displacement spectrum, and phase coherence values remained uniformly low across frequencies. Although minor SOAEs were observed in some individuals, they did not coincide with any coherence peaks, and the overall spectra were largely noisy.

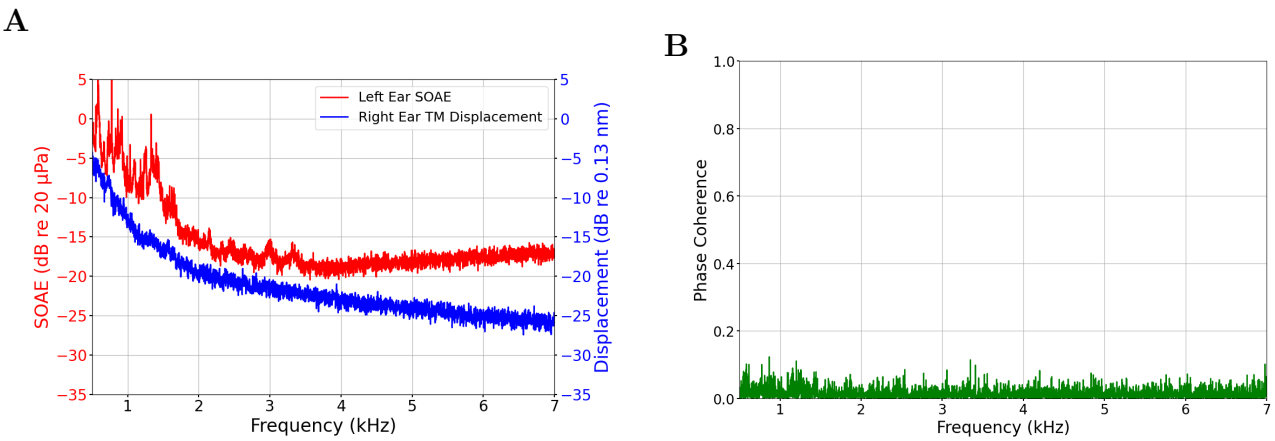

Figure 4.2: (A) Spontaneous tympanic membrane (TM) displacement (blue) and contralateral spontaneous otoacoustic emissions (SOAEs; red) recorded from a leopard gecko. The TM shows no spontaneous oscillatory activity, while the contralateral ear exhibits only minimal SOAE amplitude.(B) Corresponding phase coherence between TM motion and contralateral SOAEs, showing no distinct coherence peaks and a largely noisy spectrum, indicating the absence of interaural synchrony or coupling.

4.2 Discussion

Our findings provide compelling evidence that spontaneous TM oscillation in one ear exhibits a measurable relationship with SOAEs recorded simultaneously from the contralateral ear in the same lizard. This relationship is consistent with the notion that the lizard's middle ears interact acoustically via IAC. Here, phase coherence peaks indicate interaural synchrony between the two ears, and this supports the existence of binaural coupling. Such coupling allows spontaneous activity in one ear to influence, or be influenced by, activity in the opposite

ear. The magnitude of the coherence peaks scaled with the amplitude of TM displacement, suggesting that stronger local oscillations at distinct spectral frequencies enhance more robust synchronization across the ears. Furthermore, when SOAE peaks were present in the contralateral ear but no corresponding SO peaks were visible in the ipsilateral TM, coherence peaks were absent, suggesting that the coupling between the two ears was weak under those conditions. These findings support the idea that binaural coupling in lizards provides an acoustic feedback link between the two active inner ears, which enables the synchronization of their spontaneous activity through interactions in the IAC (Christensen-Dalsgaard & Manley, 2008; Roongthumskul et al., 2019; Bergevin et al., 2020).

While the number of leopard geckos we studied was small, the lack of detectable SO peaks in this species may point to a reduced level of active spontaneous oscillatory drive from the inner ear. This finding is consistent with prior research, which demonstrates that SOAEs in geckos are generally of lower amplitude and less prevalent than those observed in anoles (Manley and Gallo, 1996). Taken together, our results reinforce the concept that the lizard auditory system operates as a coupled bilateral oscillator, in which the active processes of each ear dynamically interact through the interaural cavity. The observed phase coherence between spontaneous TM oscillation and simultaneously recorded contralateral SOAEs thus provides direct evidence of this coupling at the level of the TM itself.

Chapter 5

Test for Nonlinearity on Tympanic Membrane Surface

Hypothesis 3: ***The TM will exhibit nonlinear mechanical behaviour to varying SPLs since OAEs reveal nonlinear acoustic responses in the ear canal***

The lizard TM, like that of mammals, vibrates in response to external sound stimuli (Manley, 1970a, 1970b). As mentioned earlier, TM responds to external stimuli and reveals how acoustic energy is transmitted as vibrations through the middle ear. As the primary interface between external sound and the inner ear, the TM's mechanical response characteristics, such as displacement amplitude, frequency dependence, and phase pattern, reveal essential information about how efficiently sound energy is transmitted and perceived. Measurement of sound evoked TM motion under controlled acoustic stimulation allows us to evaluate how effectively the TM transduces sound pressure into mechanical displacement. We quantified this input-output relationship using the transfer function (Chapter 2, section 3.2). For a linear time-invariant system, the transfer function is independent of stimulus level. In this context, it means the input pressure should scale proportionally to the TM response. In contrast, nonlinear behavior is revealed when the transfer function becomes level-dependent (e.g., changes in magnitude or phase with SPL) and/or when additional spectral components

appear that are not present in the stimulus.

Nonlinearity, a hallmark of the active mechanisms within the inner ear, plays a crucial role in amplification and fine-tuning of auditory sensitivity. Since OAEs are known to arise from such nonlinear behaviour (Kemp, 1978; Rosowski et al., 1984), analyzing the TM's mechanical response across different sound pressure levels (SPLs) allows to test whether similar nonlinear features can be detected at the level of the eardrum itself.

In this study, we therefore measured the sound-evoked response of the TM across multiple SPLs in both green anoles and leopard geckos to characterize how the mechanical response of the TM varies across species. This approach enabled us to examine whether the TM motion reflects nonlinear dynamics consistent with contributions from the active inner ear.

5.1 Result

We measured the TM's sound evoked responses in both green anoles and leopard geckos to characterize how the mechanical response of the TM varies across species and sound levels. As reported in earlier middle ear studies of lizards, both species exhibited stronger responses in the low-to-mid frequency range, followed by a steady roll-off at higher frequencies (Manley, 1972b; Saunders and Johnstone, 1972).

To test for nonlinearity, we computed the transfer function using the displacement metric (in dB re 0.13 nm/Pa) as a measure of how the TM converts incident sound pressure into mechanical motion. Because our measurement system enabled full-field mapping of the TM surface, we performed this analysis across three primary regions of the TM, dorsal, middle, and ventral, to capture regional variations in mechanical behaviour. Figure 5.1 shows a representative example from the middle region of an anole TM, illustrating the transfer function across eight sound pressure levels (SPLs) ranging from 7 to 69 dB SPL. Each coloured curve shows the magnitude in decibels relative to a reference value of 0.13 nm/Pa (i.e., dB re 0.13 nm/Pa). In this convention, 0 dB corresponds to TM displacement of 0.13

nm/Pa; values above 0 dB indicate greater displacement per unit pressure, and values below 0 dB indicate smaller displacement per unit pressure (Figure 5.1 (A)) and phase response at given SPLs (Figure 5.1(B)).

In the magnitude spectra, all curves largely overlap across frequencies, except in the lower frequency range (less than 1 kHz), where the responses do not perfectly overlap. This lack of overlap is noticeable at lower SPLs. The phase response (Figure 5.1(B)) remained relatively flat across the 0.5–8 kHz range, with minimal phase accumulation within this frequency band. At higher frequencies (>8 kHz), greater variation was observed.

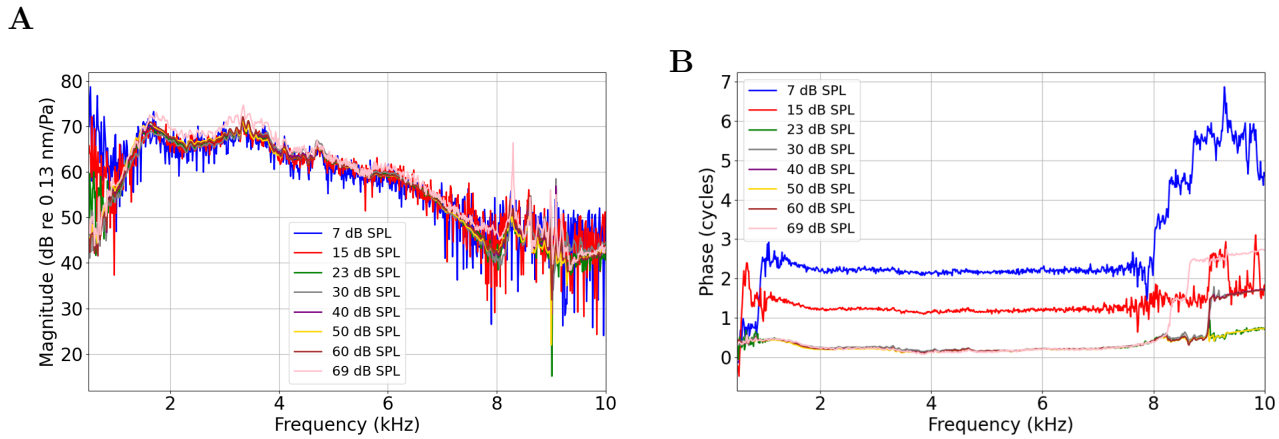

Figure 5.1: (A) Sound-evoked displacement of the TM of the green anole, expressed as transfer-function magnitude (dB re 0.13 nm/Pa) across frequencies. Each spectrum represents the TM response at a different SPL. (B)Corresponding phase responses of the TM across frequencies.

Although we tested fewer SPLs in the leopard geckos, we can nevertheless infer similar mechanical behavior from the available data. The representative example shown in Figure 5.2 (30 and 50 dB SPL) for the middle region demonstrates a comparable trend to that observed in the anole. The displacement spectra for both sound levels overlapped closely across the frequency range (0.5 - 10kHz). Likewise, the phase spectra remained relatively stable across most of the frequency band, with minor fluctuations emerging at higher frequencies. Across the remaining two primary regions analyzed (dorsal and ventral, not shown), we observed comparable magnitude patterns and spectral behaviours consistent with those seen in the

middle region for both species.

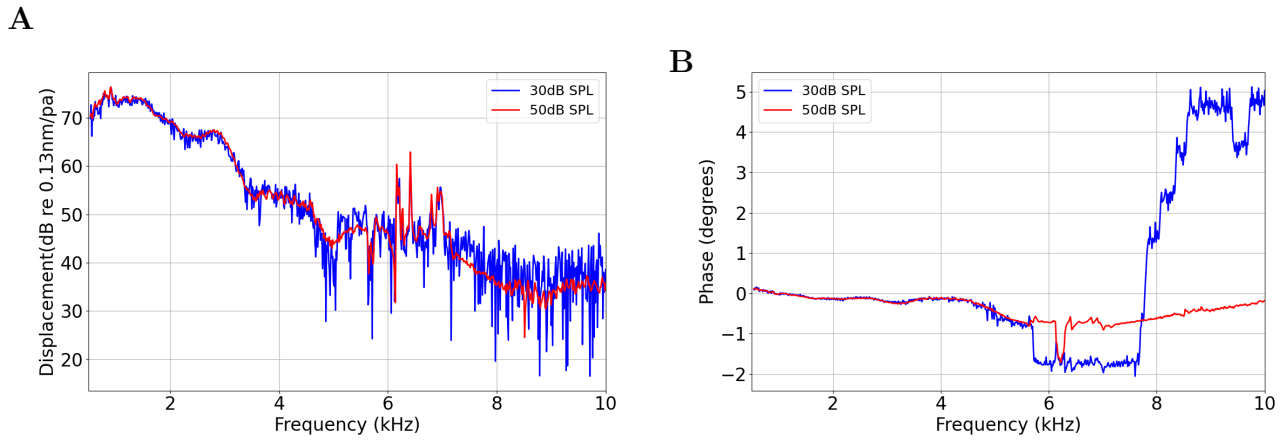

Figure 5.2: (A) Sound-evoked displacement of the TM of the leopard gecko with few SPL, expressed as transfer-function magnitude (dB re 0.13 nm/Pa) across frequencies. Each spectrum represents the TM response at a different SPL. (B)Corresponding phase responses of the TM across frequencies.

5.2 Discussion

The overlaid spectral responses across multiple SPLs indicate that the TM of both lizard species behaves linearly within the tested stimulus range. The small variations observed at low frequencies are attributed to noise rather than to real nonlinear changes in TM motion, with this noise being more evident at lower SPLs. At these levels, the sound energy delivered by the speaker was insufficient to evoke a clear mechanical response from the TM, resulting in noisier spectra. As SPL increased (above 40 dB SPL), this noisiness diminished, and the spectral curves overlaid one another, which validates that the TM's sound evoked response scaled proportionally with stimulus level.

The relatively flat phase response across most of the tested band (0.5–10 kHz) suggests that the timing of TM motion relative to the acoustic stimulus remained largely consistent across frequency. Within this range, there is no strong evidence of phase accumulation (i.e., an increasing time delay) with frequency, aside from small fluctuations above 8 kHz.

Our findings show that, under the SPLs tested, the TM exhibits a linear response, in contrast to the nonlinear mechanisms underlying otoacoustic emissions in the inner ear. In addition, the TM showed uniform linear behavior across its surface, as the dorsal, middle, and ventral regions all displayed similar magnitude and phase patterns (see Appendix A.3). These suggest that, during the forward transmission pathway, the lizard TM converts sound pressure into displacement with uniform spatial motion and minimal phase accumulation. Hence, the TM provides an effective pathway for the transmission of sound energy to the inner ear.

Chapter 6

Investigation of Hopf Bifurcation Dynamics in Tympanic Membrane Vibrations

As mentioned earlier (Chapter 1, section 1.1), cochlear amplification is one of the four features of the active process in the inner ear; others include frequency tuning, compressive nonlinearity, and SOAEs. Together, these phenomena provide evidence of the nonlinear dynamics of the inner ear (Manley, 2000, 2001). These features often occur jointly in many species and in theory, have been linked to systems operating near a Hopf bifurcation, a type of nonlinear instability that can give rise to self-sustained oscillations (Camalet et al., 2000; Eguiluz et al., 2000).

This chapter builds on the narrative from past studies by Alonso et al.(2025), who conducted ex vivo experiments on excised gerbil cochlear segments. While they reported that the four hallmarks of the active process arise from the system operating near a Hopf bifurcation, they were unable to record SOAEs in their preparation. In addition, they showed that the ear exhibits nonlinearity at low SPL in their investigation of the compressive behavior of isolated cochlear segments. They examined the cochlear microphonic responses

to single tones of varying intensity. They found that by plotting the logarithmic pressure on the horizontal axis and the TM displacement on the vertical axis, the response near the characteristic frequency (CF) revealed a pronounced compressive nonlinearity, with a slope of one-third power law predicted by the Hopf bifurcation framework. Outside of the characteristic frequency, the response was linear. In the present study, we extend this theoretical framework to a living auditory system by examining TM motion in lizards. We hypothesize that if the ear operates near a Hopf bifurcation, then the TM should also display nonlinear, level-dependent response, given that it is mechanically coupled to the inner ear and participates in the forward and reverse transmission of sound. Since our measurements are taken from living animals that exhibit spontaneous emissions, this study provides a unique opportunity to test whether TM vibrations reflect the same active nonlinear properties predicted by the Hopf framework. Hence, this analysis proceeds under the following assumptions:

- The Hopf bifurcation framework provides an appropriate description for modeling the behavior of simpler auditory systems such as lizards.
- The system exhibits spontaneous oscillations, which serve as a signature of activity near a Hopf bifurcation.
- If the measurements of these oscillations at the level of the TM are indicative of the underlying nonlinearity, then we should be able to observe the characteristic level dependence predicted by the Hopf bifurcation framework.

Based on these, we expect to observe the characteristic nonlinear level dependence predicted by the Hopf bifurcation framework in our sound evoked TM measurements.

6.1 Result

To investigate whether the TM exhibits compressive nonlinearity as predicted by the Hopf bifurcation framework, we analyzed the displacement amplitude as a function of sound pres-

sure at the frequency corresponding to a strong SO peak, plotted on a doubly logarithmic coordinate. This frequency was selected because any nonlinear behavior associated with the active process would be most pronounced at frequencies of strong spontaneous activity.As shown in Figure 6.1, displacement amplitude increases with sound pressure. A power-law fit to the data yielded a slope of n = 0.92, which indicates an almost linear relationship between sound pressure and displacement. The absence of a slope near one-third (as would be expected for a compressive nonlinearity) suggests that the TM response is approximately linear within the tested stimulus range. Minor deviations from perfect linearity at lower SPLs are due to measurement noise rather than genuine compressive nonlinear behavior.

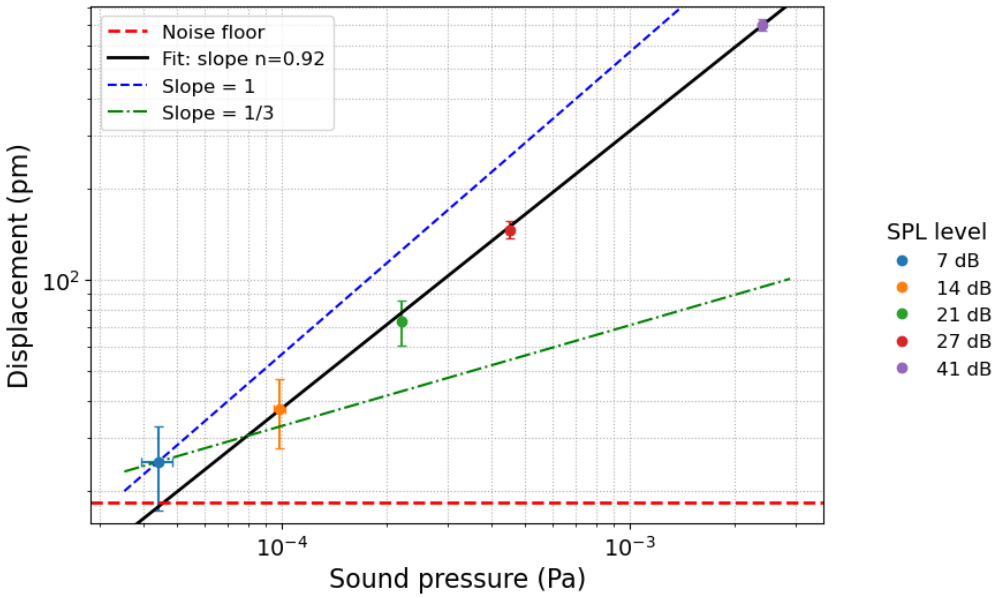

Figure 6.1: Relationship between TM displacement and sound pressure (Pa) at SO peak frequency (1.41 kHz) in the green anole shown in Chapter 4, Figure 4.1(A). Coloured data points correspond to different stimulus levels. The solid black line is a power-law fit, with n=0.92, indicating an approximately linear relationship between displacement and sound pressure. over the tested range. The dashed reference lines indicate slope n=1 (blue; perfectly linear scaling) and slope n=1/3 (green; compressive scaling). The horizontal dashed red line marks the experimental noise floor. No evidence of compressive nonlinearity (1/3-power behavior) was observed within the measured range.

6.2 Discussion

Our finding that the linear responses of the TM at low SPLs align with earlier observations by Martin and Hudspeth (2001), who investigated the mechanical responses of active hair cells from the bullfrog sacculus in an ex vivo two-chamber preparation. In their study, individual hair bundles that exhibited spontaneous oscillations responded linearly at low stimulus levels, with no evidence of the one-third power law or compressive nonlinearity predicted by the Hopf bifurcation framework. While at higher frequencies from the hair cell bundle's characteristic frequency, the responses remained linear and of constant sensitivity throughout the range of SPLs. Similar observations have been reported in in vivo studies of the mammalian cochlea. For example, Ruggero et al. (1997), Overstreet et al. (2002), and Chen et al. (2011) demonstrated that basilar membranes are linear at low SPLs, and only exhibit nonlinear compressive behavior as stimulus levels increase. Comparable findings have also been observed at the level of the TM across species. For instance, Rosowski et al. (1984b), measured the acoustic input admittance of the alligator lizard ear across multiple SPLs and found that the TM response was linear at low levels, while nonlinear variations emerged above 65 dB SPL. Similarly, Dalhoff et al. (2007) reported linear responses of in vivo measurements of the human TM down to 20 dB SPL. Consistent with earlier results, our measurements reveal that the TM remains linear even at very low SPL around 7 dB SPL, with no evidence of nonlinear behaviour. These results challenge one of the central predictions of the Hopf bifurcation framework, which proposes that compressive nonlinearity should emerge at low SPLs as a manifestation of active cochlear amplification. In contrast, our measurements suggest that, at the level of the TM, responses remain linear. In addition, our observation of SO and SOAEs reveals the sensitivity of the lizard ear. The fact that the TM exhibits measurable motion even in the absence of external sound stimuli reflects the presence of active mechanical processes that operate within the auditory system.

Chapter 7

Comparison of Experimental Data with Previous Studies

Before making comparisons with earlier studies, we assessed the accuracy and repeatability of our experimental measurements. This step ensured that any differences or similarities observed with earlier work could be attributed to biological or methodological factors, rather than variability within our dataset. To do this, we assessed two key aspects of data integrity: (1) the repeatability of our TM measurements over time and (2) the potential influence of contralateral ear occlusion on the sound-evoked responses of the ipsilateral TM.

7.1 Repeatability Test of Spontaneous and Sound Evoked TM Measurements

It has been well documented that SOAEs in lizards are inherently unstable and can fluctuate over time (Manley et al., 2006). Consistent with previous reports of spontaneous activity instability in lizards, our repeated spontaneous measurements, which compared the TM's spontaneous oscillations and the contralateral SOAEs measured two weeks apart (Figure 7.1), showed noticeable spectral variations between sessions. While the overall spectral

shape remained similar, the repeated SO measurement showed reduced peaks as compared to the initial measurements, along with small frequency shifts and fewer distinct SOAE peaks. Fluctuations in spontaneous activity are expected due to physiological and temperature changes. Despite this variability, the overall spectral pattern of our spontaneous measurements was repeatable.

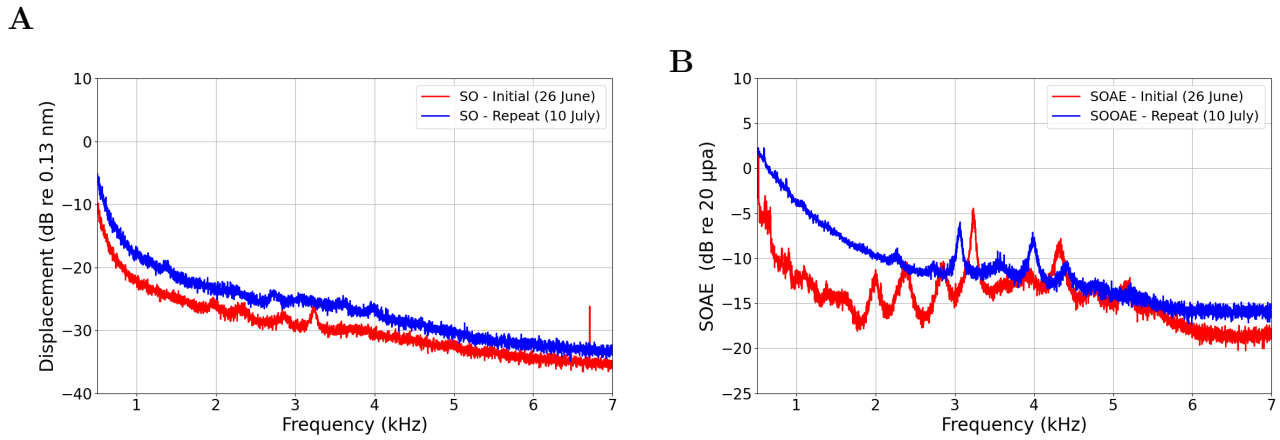

Figure 7.1: (A) Initial (red) and repeated (blue) spontaneous oscillations of the same TM measured two weeks apart in an anole. (B) Corresponding SOAEs recorded from the contralateral ear during the same sessions. Both panels illustrate changes in spectral amplitude and frequency structure between sessions.

In contrast, the sound-evoked measurements demonstrated temporal stability (Figure 7.2). To evaluate repeatability, we conducted repeated single-point TM measurements in the same animal (anole) at 27 dB SPL, recorded twice at 15-minute intervals under identical measurement settings. As shown in Figure 7.2, the magnitude and phase spectra from the initial and repeated measurements overlapped across the frequency range. This confirms the repeatability of our sound-evoked measurements.

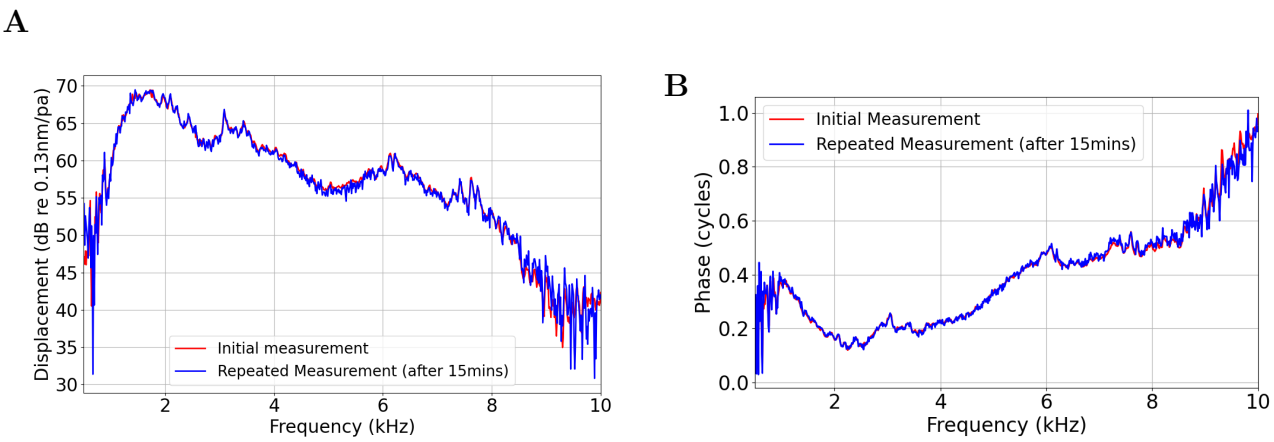

Figure 7.2: (A) Initial (red) and repeated (blue) sound evoked transfer function displacement of the same TM measured 15 minutes apart in an anole. (B) Corresponding phase of the TM response. Both panels demonstrate temporal stability and repeatability of the measurements.

7.1.1 Effect of Contralateral Ear Coupling on Ipsilateral TM Response

Having confirmed the repeatability of our measurements, we next examined how experimental conditions might influence the TM response. One key methodological factor to address before comparing our data with previous studies is the effect of contralateral ear occlusion. Unlike earlier studies in which the contralateral ear was left open during sound-evoked measurements (e.g., Manley, 1972; Christensen-Dalsgaard, 2005, 2008), our experimental setup involved coupling the contralateral ear with a probe microphone. Evaluating whether this difference affects the measured TM response is therefore crucial to ensure that subsequent comparisons across studies are unbiased and physiologically meaningful.

To assess this, we compared the sound-evoked TM vibration under two conditions: when the contralateral ear was unsealed and when it was sealed, across both species (Figure 7.3). The results show that the transfer function magnitude and phase of the ipsilateral TM were similar across the two conditions. The spectral profile overlapped in both species with no significant differences across the frequency range.

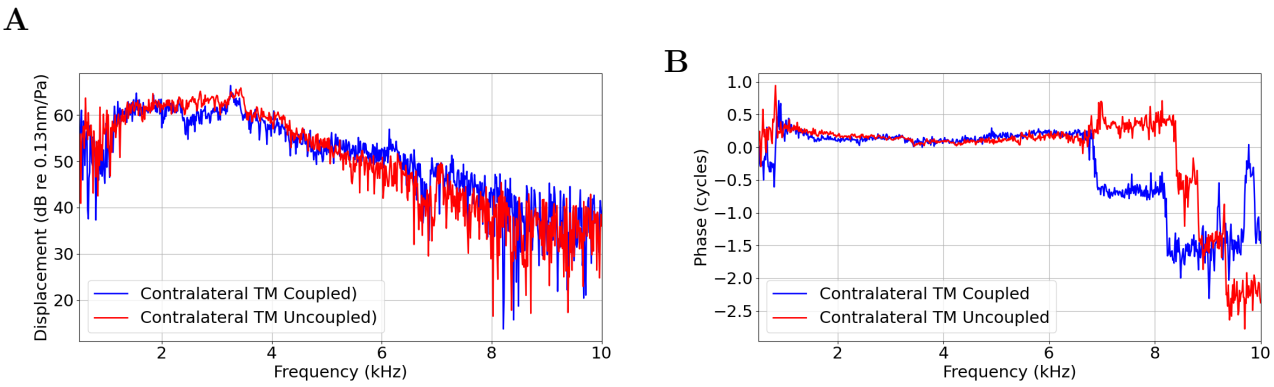

Figure 7.3: (A) Sound evoked transfer function displacement of the ipsilateral TM with the contralateral ear coupled (blue) and uncoupled (red), measured at 8 dB SPL. (B) Corresponding phase of the TM transfer function. The results reveal no significant variation between the two measurement conditions.

These results confirm that coupling the contralateral ear has no measurable impact on the TM's sound evoked vibration. As such, our data can be reliably compared with earlier studies performed under open contralateral ear conditions. Below are the various comparisons with previous data that we made.

7.1.2 Manley 1972

In this classical study, Manley (1972) measured the absolute sound evoked response of the TM in the Tokay gecko using the Mössbauer technique at a stimulus level of 100 dB SPL to measure the TM velocity. When compared with our data, both our leopard gecko results and Manley's measurements a similar displacement spectral shape, characterized by higher amplitudes at lower frequencies and a gradual decline toward higher frequencies. However, the displacement magnitudes observed in our measurements are higher than those reported by Manley, which may reflect interspecific differences between leopard and tokay gecko, as well as differences in measurement sensitivity between the two techniques.

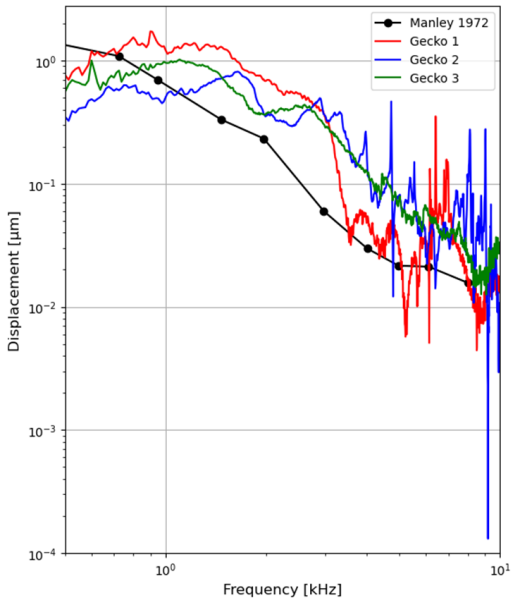

Figure 7.4: Comparison of TM displacement spectra between the present study and Manley (1972). Across the frequency range, the displacement magnitudes observed in this study are comparable to Manley's data, showing similar higher responses at low frequencies and a gradual decline toward higher frequencies.

7.1.3 Christensen-Dalsgaard (2005)

We also compared our results with a more recent study by Christensen-Dalsgaard (2005), who used laser Doppler vibrometry to measure the TM velocity in the Tokay gecko. In this comparison, we examined the transfer function displacement metric from our leopard gecko measurements alongside the Tokay gecko data reported by Christensen-Dalsgaard, which we converted to displacement. As shown in Figure 7.5, both datasets show similar frequency-dependent patterns, with higher magnitude at lower frequencies and a gradual decline at higher frequencies. However, our leopard gecko measurements exhibit greater overall motion amplitudes compared to the Tokay gecko results, which could reflect interspecific differences and sound pressure calibration.

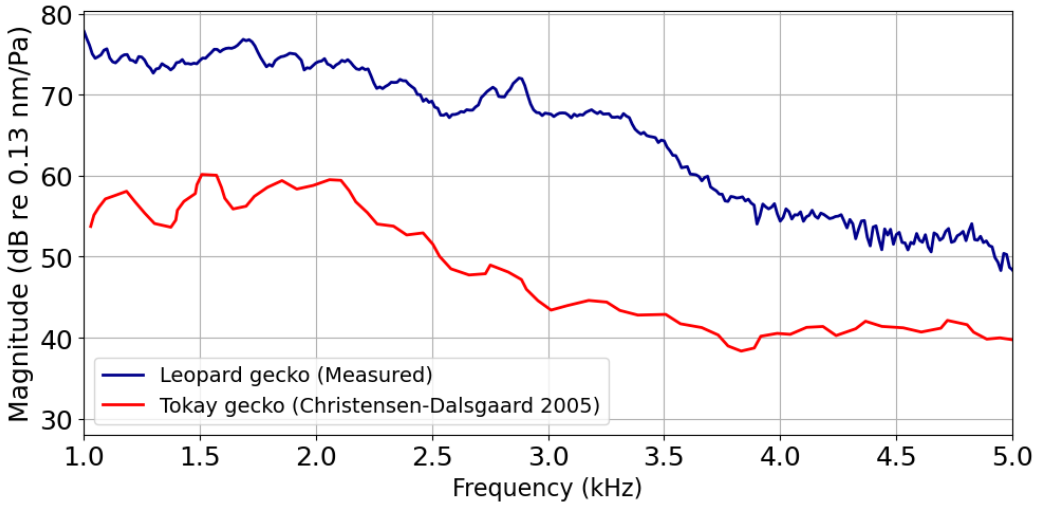

Figure 7.5: Comparison of TM velocity transfer functions between the leopard gecko (present study) and the Tokay gecko reported by Christensen-Dalsgaard (2005).

7.1.4 Christensen-Dalsgaard and Manley (2008)

Using the Anolis species, we further compared our results with the TM transfer function velocity measurements reported by Christensen-Dalsgaard and Manley (2008), shown in Figure 7.6. In their study, TM motion was recorded under two acoustic stimulation conditions: ipsilateral stimulation, where the loudspeaker was positioned on the same side as the measured TM, and contralateral stimulation, where the loudspeaker was placed on the opposite side, and the TM motion was measured in response to sound presented to the other ear. This pattern shows how the two eardrums interact acoustically; sound coming through one ear can set the opposite TM into motion, although the response is weaker because some energy is lost as it travels through the interaural cavity.

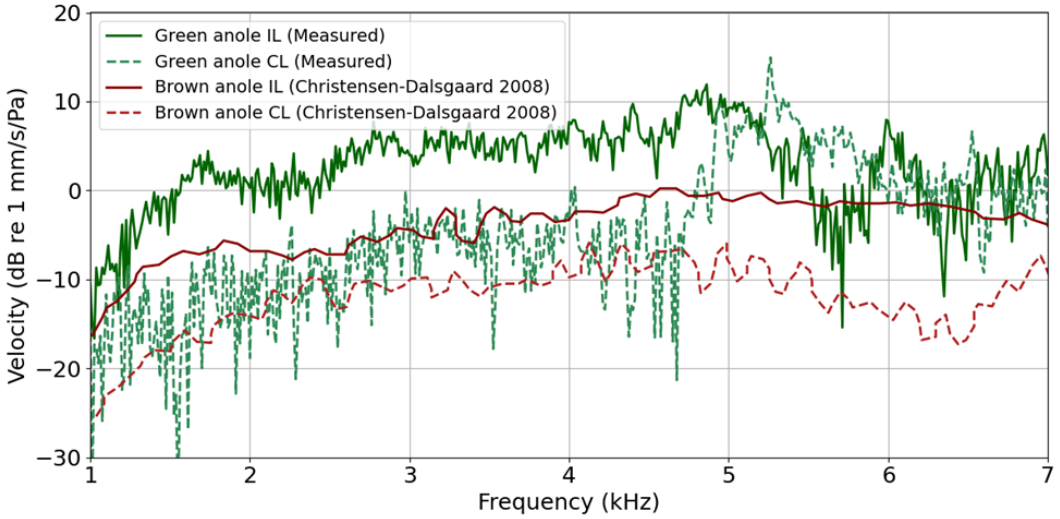

Figure 7.6: Comparison of TM velocity transfer functions between the green anole (present study) and the brown anole reported by Christensen-Dalsgaard (2008)

Chapter 8

Final Discussion, Summary and Conclusions

8.1 Overview and Rationale

The focus of this thesis was to characterize how both externally evoked sounds and internally generated SOAEs drive TM vibrations, with a broader goal of understanding the active inner-ear processes that underlie otoacoustic emissions (OAE) generation. While the long term aim of studying OAEs is to better understand the human auditory system, conducting this research in non-mammalian vertebrates such as lizards, which emit robust OAEs and have a relatively simpler auditory system that nonetheless functions well for hearing is very informative.

Here, we studied the auditory periphery of lizards (green anole and leopard gecko) at the level of the tympanic membrane (TM), a middle-ear structure that serves two roles. In forward transmission, it is the first stage that converts airborne sound pressure into mechanical vibrations that are transmitted to the inner ear and ultimately to the brain. In backward transmission, it is the final stage through which sound energy originating in the inner ear is converted into acoustic pressure in the ear canal, where it can be measured as

OAEs.

Using a scanning laser Doppler vibrometer (sLDV,) we measured TM vibrations in response to external sound, and in the absence of external stimulation, where motion is driven by active forces from the inner ear. Using a sensitive microphone probe, we simultaneously recorded spontaneous otoacoustic emissions (SOAEs) from the contralateral ear.

8.2 Summary of Main Findings

1. **Picometer-scale pontaneous TM Motion (see chapter 2).**

   Spontaneous displacement of the TM due to inner-ear activity was detected at subatomic scales (picometer-level), smaller than the diameter of a hydrogen atom.

2. **Evidence consistent with interaural coupling during spontaneous activity (see chapter 3).**

   We found that the spectral features of spontaneous TM oscillations measured in one ear and the simultaneously recorded acoustic signal (SOAE) from the contralateral ear largely matched, consistent with binaural synchronization between ears.

   Although humans do not possess an interaural cavity, the broader idea of binaural synchrony remains relevant. Insights from coupled two-ear systems may inform engineering strategies in which bilateral hearing devices (e.g., paired hearing aids or cochlear implants) exchange information to improve sound localization for the wearer.

3. **Sound-evoked TM motion was approximately linear near threshold levels (see chapter 6).**

   For sound-evoked measurements, TM motion behaved approximately linearly within the stimulus range (7dB-65 dB SPL) examined. In particular, the displacement–pressure relationship did not exhibit evidence of compressive scaling near threshold levels.

4. **Relatively flat phase across frequencies (see chapter 6).**

Classical membrane theory (e.g., Fletcher 1992) and more recent theoretical models of the reptilian tympanum (Vedurmudi et al. 2016b) predict that with increasing frequency, the TM will switch vibratory modes, and that this switch will be marked by a more asymmetric response. In our measurements, however, the phase of the sound-evoked response remained relatively flat across most of the tested bands, with no evidence of phase accumulation. This suggests that, within the measured bandwidth across the visible surface of the TM, the dominant phase behavior of TM motion did not change with frequency.

8.3 Limitations

1. **Absence of reflectivity enhancement on the TM surface.**

   In this study, we did not apply reflective material to the visible TM surface. Because LDV sensitivity depends on optical return, limited reflectivity is one of the factors that increases the noise floor at some locations, and this reduces the detectability of low-amplitude spontaneous motion. Future work could improve measurement sensitivity by enhancing surface reflectivity, which would improve the signal-to-noise ratio (SNR) and reduce the noise floor.

2. **Differences in coupling conditions between measurements.**

   As mentioned earlier in this study, the microphone probe was closely coupled to the TM to record SOAE, while the simultaneous measurement of the spontaneous oscillation of the TM was conducted without any coupling. The differences in both measurement conditions influence the acoustic loading, which could affect the vibration profile. Future studies should have similar coupling conditions across acoustic and mechanical measurements to enable more direct comparison of the spectra.

8.4 Concluding Remarks

In conclusion, the results obtained from this research will help inform theories of how the inner ear achieves its remarkable functionality and how the two ears can cooperatively work together binaurally in non-mammals such as lizards.

Bibliography

[1] Araújo, L. C., Magalhaes, T. N., Souza, D. P., Yehia, H. C., & Loureiro, M. A. (2005). A brief history of auditory models. 10 Simpósio Brasileiro de Computaçao Musical, 1.

[2] Baird, I. L. (1970). The anatomy of the reptile ear. In: C. Gans & T. S. Parsons (Eds.), Biology of the Reptilia, Vol. 2. New York: Academic Press, pp. 193–275.

[3] Bergevin, C., Freeman, D. M., Saunders, J. C., & Shera, C. A. (2008). Otoacoustic emissions in humans, birds, lizards, and frogs: evidence for multiple generation mechanisms. Journal of Comparative Physiology A, 194(7):665–683.

[4] Bergevin, C., Walsh, E. J., McGee, J., & Shera, C. A. (2012). Probing cochlear tuning and tonotopy in the tiger using otoacoustic emissions. Journal of Comparative Physiology A, 198(8), 617-624.

[5] Bergevin, C., Mhatre, N., & Mason, A. (2018). Comparing external tympanic vibration and spontaneous otoacoustic emissions. AIP Conference Proceedings, 1965, 130004.

[6] Bergevin, C., Mason, A., & Mhatre, N. (2020). Evidence supporting synchrony between two active ears due to interaural coupling. Journal of the Acoustical Society of America, 147(1): EL25–EL31.

[7] Brittan-Powell, E. F., Tang, Y., Christensen-Dalsgaard, J., & Carr, C. E. (2010). The auditory brainstem response in two lizard species. Journal of the Acoustical Society of America, DOI: 10.1121/1.3458813.

[8] Camalet, S., Duke, T., Jülicher, F., & Prost, J. (2000). Auditory sensitivity provided by self-tuned critical oscillations of hair cells. Proceedings of the National Academy of Sciences U.S.A., 97, 3183–3188.

[9] Chen, F., Zha, D., Fridberger, A., Zheng, J., Choudhury, N., Jacques, S. L., Wang, R. K., Shi, X., Nuttall, A. L., & Wang, R. K. (2011). A differentially amplified motion in the ear for near-threshold sound detection. Nature Neuroscience, 14, 770–774.

[10] Cheng, J. T., Antti, A. A., Ellery, H., Hernandez-Montes, M. S., Cosme, F., Saumil, N. M., & Rosowski, J. J. (2009). Motion of the surface of the human tympanic membrane measured with stroboscopic holography. Hearing Research, 263, 66–77.

[11] Cheng, J. T., Harrington, E., Horwitz, R., Furlong, C., & Rosowski, J. J. (2011). The Tympanic Membrane Motion in Forward and Reverse Middle-Ear Sound Transmission. In AIP Conference Proceedings (Vol. 1403, No. 1, pp. 521-527). American Institute of Physics.

[12] Cheng, J. T., Maftoon, N., Guignard, J., Ravicz, M. E., & Rosowski, J. (2019). Tympanic membrane surface motions in forward and reverse middle ear transmissions. The Journal of the Acoustical Society of America, 145(1), 272-291.

[13] Christensen-Dalsgaard, J., & Manley, G. A. (2005). Directionality of the lizard ear. Journal of Experimental Biology, 208(6):1209–1217.

[14] Christensen-Dalsgaard, J., & Manley, G. A. (2008). Acoustical coupling of lizard eardrums. Journal of the Association for Research in Otolaryngology, 9, 407–416.

[15] Dalhoff, E., Turcanu, D., Zenner, H. P., & Gummer, A. W. (2006). Distortion product otoacoustic emissions measured as vibration on the eardrum of human subjects. Proceedings of the National Academy of Sciences U.S.A., 103, 1546–1551.

[16] Dallos, P. (2008). Cochlear amplification, outer hair cells and prestin. Current opinion in neurobiology, 18(4), 370-376.

[17] Eguiluz, V. M., Ospeck, M., Choe, Y., Hudspeth, A. J., & Magnasco, M. O. (2000). Essential nonlinearities in hearing. Physical Review Letters, 84, 5232–5235.

[18] Fletcher NH (1992) Acoustic systems in biology. Oxford University Press, New York.

[19] Fetiplace, R. (2020). Diverse mechanisms of sound frequency discrimination in the vertebrate cochlea. Trends in Neurosciences, 43, 88–102. Gelfand, M., Piro, O., Magnasco, M. O., & Hudspeth, A. J. (2010). Interactions between hair cells shape spontaneous otoacoustic emissions in a model of the Tokay gecko's cochlea. PLoS ONE, 5(6): e11116.

[20] Gatzwiller, K. B., Ginn, K. B., Betts, A., & Morel, S. (2002). Practical aspects of successful laser doppler vibrometry based measurements. In Proceedings of 21 st International Modal Analysis Conference (IMAC-XXI), Kissimmee, Florida. changes in physiological states. Biomedical Signal Processing and Control (Vol. 7, No. 4, p. 315).

[21] Gentil, F., Jorge, R.N., Ferreira, A.J.M., Parente, M.P.L., Moreira, M., Almeida, E., (2005). Biomechanical study of middle ear. In: Proceedings of the VIII International Conference on Computational Plasticity, pp. 785–788.

[22] Goode, R. L., Ball, G., & Nishihara, S. (1993). Measurement of umbo vibration in human subjects—methods and possible clinical applications. American Journal of Otology, 14, 247–251.

[23] Han, D., & Young, B. A. (2018). Biophysical heterogeneity in the tympanic membrane of the Asian water monitor lizard, Varanus salvator. Zoomorphology, 137(2), 337-348.

[24] Hudspeth, A. J. (2014). Integrating the active process of hair cells with cochlear function. Nature Reviews Neuroscience, 15(9), 600-614.

[25] Japatti, S. R., Engineer, P. J., Reddy, B. M., Tiwari, A. U., Siddegowda, C. Y., & Hammannavar, R. B. (2018). Anthropometric assessment of the normal adult human ear. Annals of maxillofacial surgery, 8(1), 42-50.

[26] Kemp, D. T. (1978). Stimulated acoustic emissions from within the human auditory system. The Journal of the Acoustical Society of America, 64(5), 1386-1391.

[27] Kemp, D. (1979). Evidence of Mechanical Nonlinearity and Frequency Selective Wave Amplification in the Cochlea. Arch. Oto-Rhino-Laryngol., 224(1-2):37–45.

[28] Kjer, H. M., Fagertun, J., Vera, S., Gil, D., Ballester, M. Á. G., & Paulsen, R. R. (2016). Free-form image registration of human cochlear CT data using skeleton similarity as anatomical prior. Pattern Recognition Letters, 76, 76-82.

[29] Manley, G. A. (1972a). The middle ear of the Tokay gecko. Journal of Comparative Physiology, 81, 239–250.

[30] Manley, G. A. (1972b). Frequency response of the middle ear of geckos. Journal of Comparative Physiology, 81, 251–258. DOI: 10.1007/BF00693630.

[31] Manley, G. A. (1990). Peripheral Hearing Mechanisms in Reptiles and Birds. ISBN 3-540-50350-1 Springer-Verlag.

[32] Manley, G. A. (2000). Cochlear mechanisms from a phylogenetic viewpoint. Proceedings of the National Academy of Sciences U.S.A., 97, 11736–11743.

[33] Manley, G. A. (2001). Evidence for an active process and a cochlear amplifier in non-mammals. Journal of Neurophysiology, 86, 541–549.

[34] Manley, G. A. (2006). Spontaneous otoacoustic emissions from free-standing stereovillar bundles of ten species of lizard with small papillae. Hearing Research, 212, 33–47.

[35] Manley, G. A., & Köppl, C. (2008). What have lizard ears taught us about auditory physiology?. Hearing research, 238(1-2), 3-11.

[36] Manley, G. A., Gallo, L., & Köppl, C. (1996). Spontaneous otoacoustic emissions in two gecko species, Gekko gecko and Eublepharis macularius. Journal of the Acoustical Society of America, 99(3):1588–1603.

[37] Manley, G. A., Köppl, C., & Sneary, M. (1999). Reversed tonotopic map of the basilar papilla in Gekko gecko. Hearing Research, 131, 107–116. Martin, P., & Hudspeth, A. J. (2001). Compressive nonlinearity in the hair bundle's active response to mechanical stimulation. Proceedings of the National Academy of Sciences U.S.A., 98, 14386–14391.

[38] Mansour, S., Magnan, J., Haidar, H., Nicolas, K., & Louryan, S. (2016). Comprehensive and clinical anatomy of the middle ear.Springe

[39] Miller, M. R. (1981). Scanning electron microscope studies of the auditory papillae of some iguanid lizards. American Journal of Anatomy, 162(1):55–72.

[40] Natarajan, N., Batts, S., & Stankovic, K. M (2023). Noise-Induced Hearing Loss. Journal of Clinical Medicine, 12(6), 2347. https://doi.org/10.3390/jcm12062347

[41] Negandhi, J., Bergevin, C., & Harrison, R. V. (2018). Scanning electron microscopy of the basilar papilla of the lizard Anolis carolinensis. Canadian Acoustics, 46(1):7–12.

[42] Overstreet III, E. H., Temchin, A. N., & Ruggero, M. A. (2002). Basilar membrane vibrations near the round window of the gerbil cochlea. Journal of the Association for Research in Otolaryngology, 3, 351–361.

[43] Puria, S. (2003). Measurements of human middle ear forward and reverse acoustics: Implications for otoacoustic emissions. Journal of the Acoustical Society of America, 113, 2773–2789.

[44] Roongthumskul, Y., Maoil'eidigh, D. Ó., & Hudspeth, A. J. (2019). Bilateral spontaneous otoacoustic emissions show coupling between active oscillators in the two ears. Biophysical Journal, 116(10):2023–2034.

[45] Rosowski, J. J., Peake, W. T., & Lynch, T. J. (1984a). Acoustic input admittance of the alligator lizard ear: Nonlinear features. Hearing Research, 16, 205–223.

[46] Rosowski, J. J., Peake, W. T., & White, J. R. (1984b). Cochlear nonlinearities inferred from two-tone distortion products in the ear canal of the alligator lizard. Hearing Research, 13, 141–158.

[47] Ruggero, M. A., Rich, N. C., Recio, A., Narayan, S. S., & Robles, L. (1997). Basilar-membrane responses to tones at the base of the chinchilla cochlea. Journal of the Acoustical Society of America, 101, 2151–2163. Saunders, J. C., & Johnstone, B. M. (1972). A comparative analysis of middle ear function in non-mammalian vertebrates. Acta Otolaryngologica (Stockh.), 73, 353–361.

[48] Vedurmudi A, Young BA, van Hemmen JL (2016b) Internally coupled ears: mathematical structures and mechanisms underlying ICE. Biol Cyber. https ://doi.org/10.1007/s0042 2-016-0696-4

[49] Vilfan, A., & Duke, T. (2008). Frequency clustering in spontaneous otoacoustic emissions from a lizard's ear. Biophysical Journal, 95(10):4622–4630.

[50] Wei, D., & Olson, E. S. (2006). Middle ear forward and reverse transmission in the gerbil. Journal of Neurophysiology, 95, 2951–2961.

[51] Werner, Y. L., & Wever, E. G. (1972). The function of the middle ear in lizards: Gekko gecko and Eublepharis macularius. Journal of Experimental Zoology, 179, 1–16.

[52] Wever, E. G. (1978). The Reptile Ear. Princeton University Press, Princeton, NJ.

[53] Wever, E. G., / Lawrence, M. (1954). Physiological acoustics.

[54] Wiley R.E., Ledo F., Fedoryk O., Bergevin C. (2025). Synchronization of two active ears via binaural coupling (Submitted).

Appendix A

Supplementary Information

A.1 Estimate of the TM Scan Point Spacing

We obtained an anatomical estimate of the TM surface area using a publicly available micro-CT data from DigiMorph (specimen:*Anolis carolinensis*) and inspected the coronal slices of the head, where we obtained the TM area A to be approximately 2.5 mm^2. Figure A.1 shows an example slice used for measurement. This area estimate was then used to approximate the average point-to-point spacing of the sLDV measurement grid. For instance, using the number of scan points, N = 50, from our sLDV measurement, we estimated the point spacing in the next section.

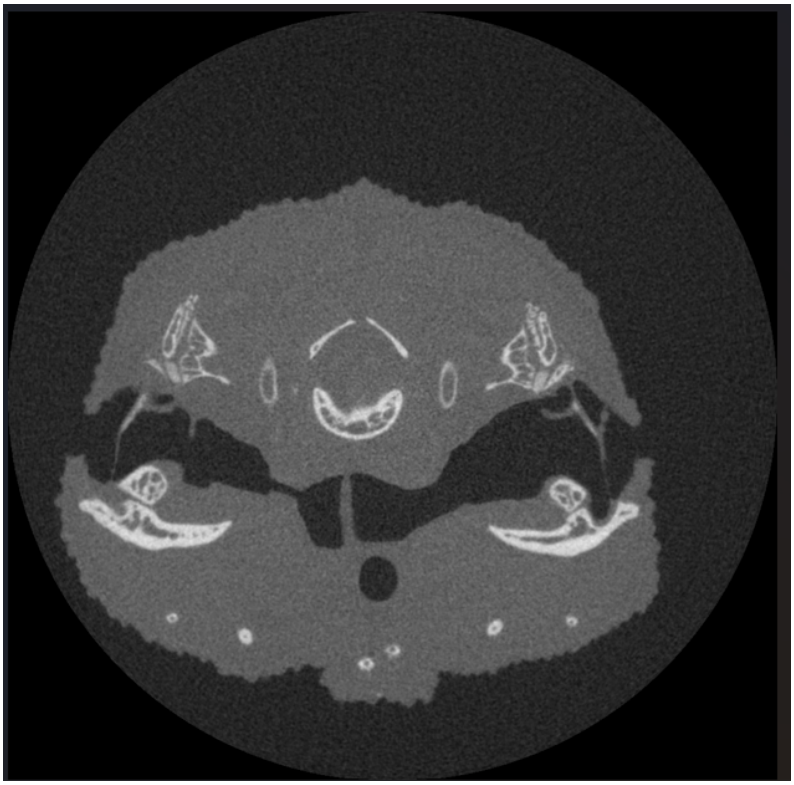

Figure A.1: Coronal micro-CT slice of *Anolis carolinensis* from DigiMorph.

A.1.1 Spacing Estimate

$$Spacing \approx \sqrt{\frac{A}{N}} = \sqrt{\frac{2.5}{50}} = \sqrt{0.05 \text{ mm}^2} \approx 0.224 \text{ mm} \approx 0.22 \text{ mm}. \tag{A.1}$$

Therefore, the scan-point spacing is estimated to be approximately 0.22 mm.

A.2 SOAE Spectra in Right versus Left Ear

Similar to the comparison between the left and right ear spontaneous oscillations in the same lizard (Chapter 2), we also compared the SOAEs recorded from each ear. As shown in figure A.2, the spectra show a slight frequency shift between the two ears, and the SOAE peaks do not perfectly align except at 3.3kHz. As mentioned earlier, we interpret these shifts to be from temperature induced changes.

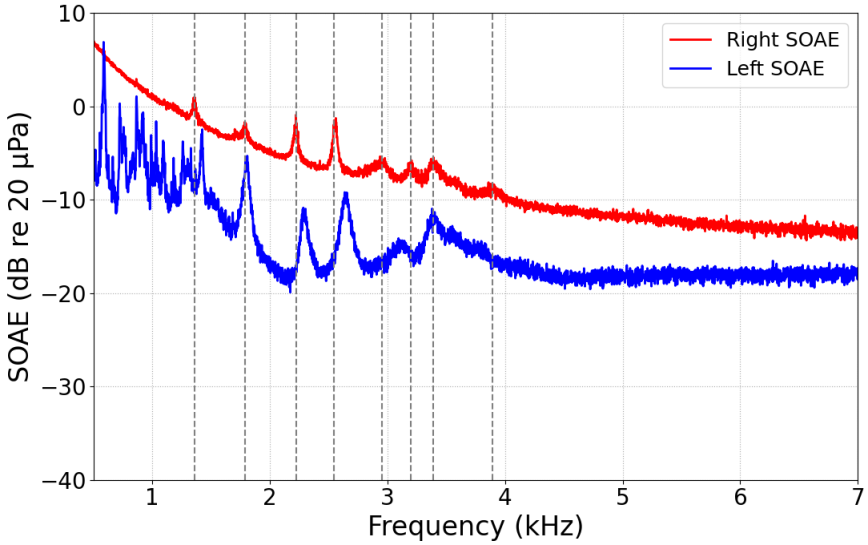

Figure A.2: Comparison between right and left SOAE spectra recorded two hours apart in the same lizard. Vertical dashed lines mark peak frequencies identified in the right-ear spectrum and are shown to facilitate comparison with the left-ear spectrum.

A.3 Spatial Nonlinearity Test on TM Surface

The nonlinearity investigation across the remaining two regions (ventral and dorsal; the middle region was shown in Chapter 3) revealed similar results to those observed in the middle region. The TM spectra at each of the regions overlapped, indicating an overall linear response. As stated earlier, the variation at the lowest SPLs are attributed to measurement noise. Overall, the displacement magnitudes across all three regions were relatively similar, and the phase responses were flat, with small fluctuations consistent with noise. These findings suggest that there are no significant spatial variations in linearity across the TM surface.

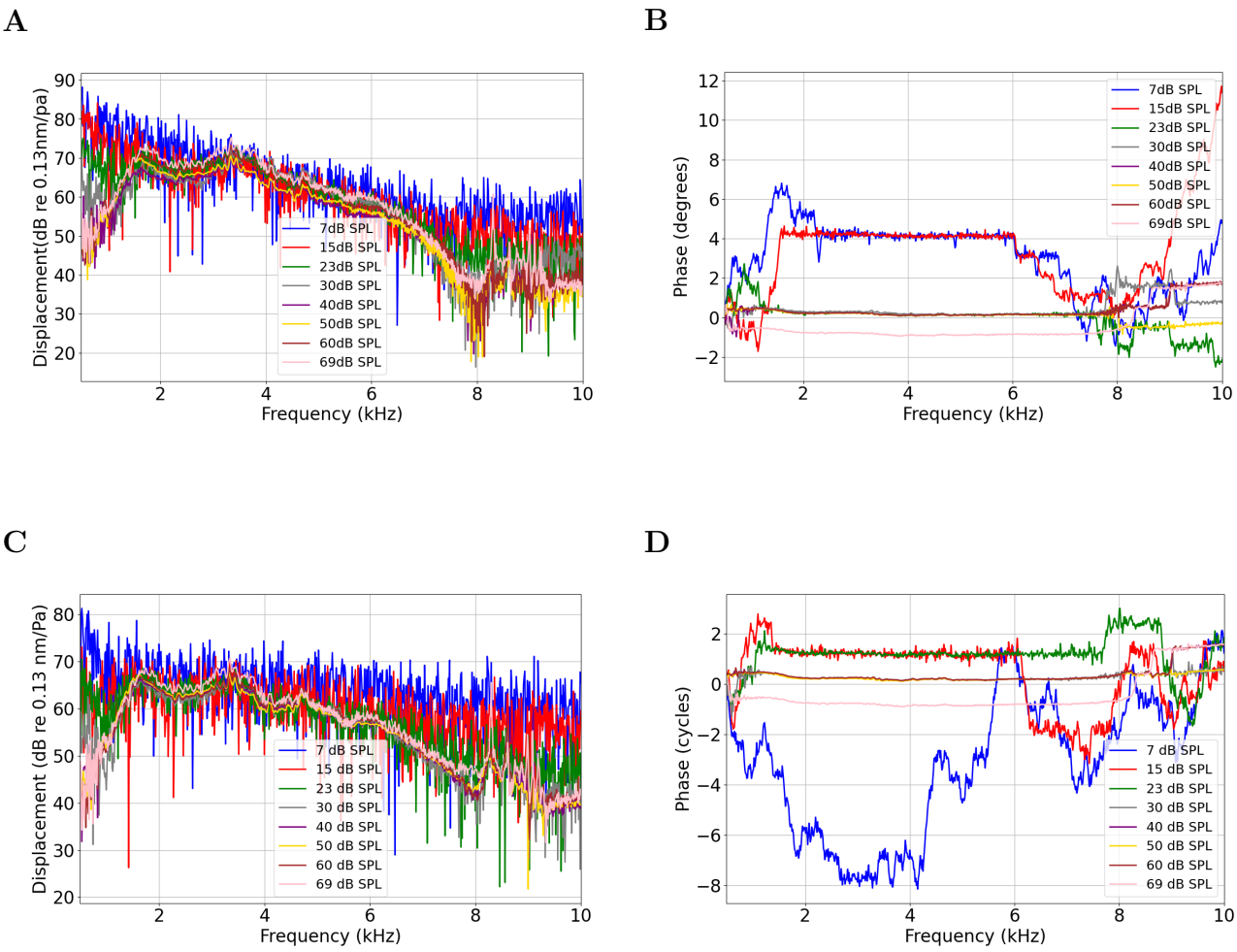

Figure A.3: (A) Displacement relative to SPL (dB re 0.13nm/Pa) at the ventral region of the TM surface. (B) Corresponding phase of the ventral region. (C) Displacement relative to SPL (dB re 0.13nm0.13 nm/Pa) the dorsal region of the TM surface. (D) Corresponding phase of the dorsal region.

A.4 Temporal Averaging and Noise Floor Dynamics

As mentioned earlier, we performed spectral averaging on the spontaneous data, as it is more effective for revealing narrow peaks than temporal averaging. Across all our measurements, an important question arises: how precisely do we know our noise floor? To explore this, we carried out a computational experiment to gain insight into the spectral dynamics of temporal averaging applied to spontaneous emissions in both lizards and human SOAE time waveforms.The goal was to determine whether there is a lower limit to how much temporal averaging can reduce the experimental noise floor, to identify the factors that set this limit, to determine whether SOAE peaks remain stable or become distorted, and to understand how increasing the temporal averaging value affects the visibility of peaks in the temporally averaged spectra.

We analyzed both short (2-minute) waveforms from lizards and humans, as well as a longer 30-minute waveform from human subjects.In the short recordings for both lizard and human, we observed that at small temporal averaging values (e.g., M = 10), the noise floor remained high, and several peaks that correspond to the SOAE peaks on the spectral averaged spectrum were still visible. As the temporal averaging increased, the noise floor progressively decreased. However, although some peaks persisted across different averaging levels, others gradually reduced in amplitude or disappeared entirely as M increased.

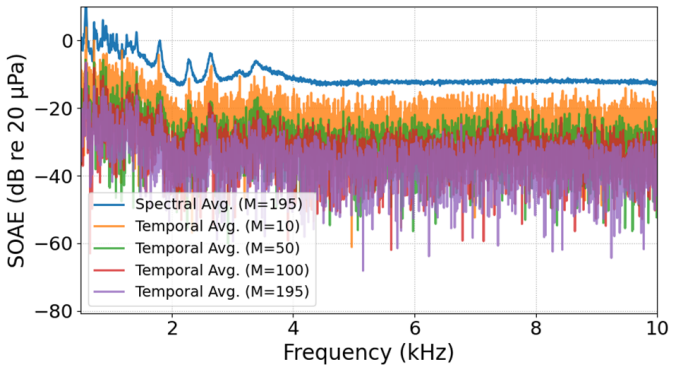

Figure A.4: Anole two-minute time waveform with spectral averaged spectra(blue) and temporal averaged spectra(each color represent different averaging values)

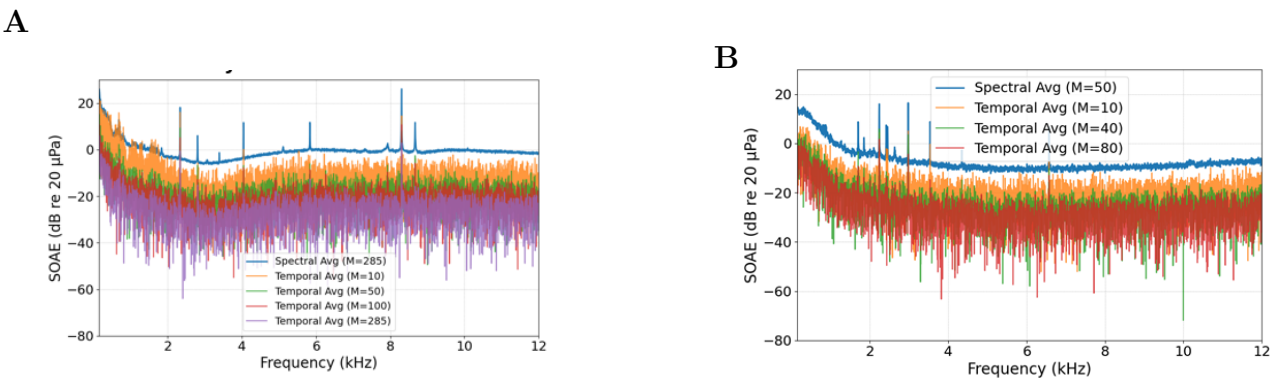

Figure A.5: Human two-minute time waveform. (A) Subject 1 (B) Subject 2.

In the short recordings for both lizard and human, we observed that at small temporal averaging values (e.g., M = 10), the noise floor remained high, and several peaks that correspond to the SOAE peaks on the spectral averaged spectrum were still visible. As the temporal averaging increased, the noise floor progressively decreased. However, although some peaks persisted across different averaging levels, others gradually reduced in amplitude or disappeared entirely as M increased.

To further investigate this behaviour, we examined a much longer 30-minute human recording, which provided a larger number of independent FFT segments. This spectra showed the same general behavior as the short recordings: temporal averaging lowered the noise floor, and some peaks remained stable, while others diminished with increasing M.Overall, our results indicate that increasing temporal averaging lowers the noise floor, but this comes with a trade-off; peaks with lower signal strength may disappear at high averaging values. The extent to which the noise floor can be lowered depends strongly on the duration of the waveform and the number of independent segments available. Thus, while higher averaging improves noise suppression, it can negatively impact the visibility of weaker spontaneous peaks.

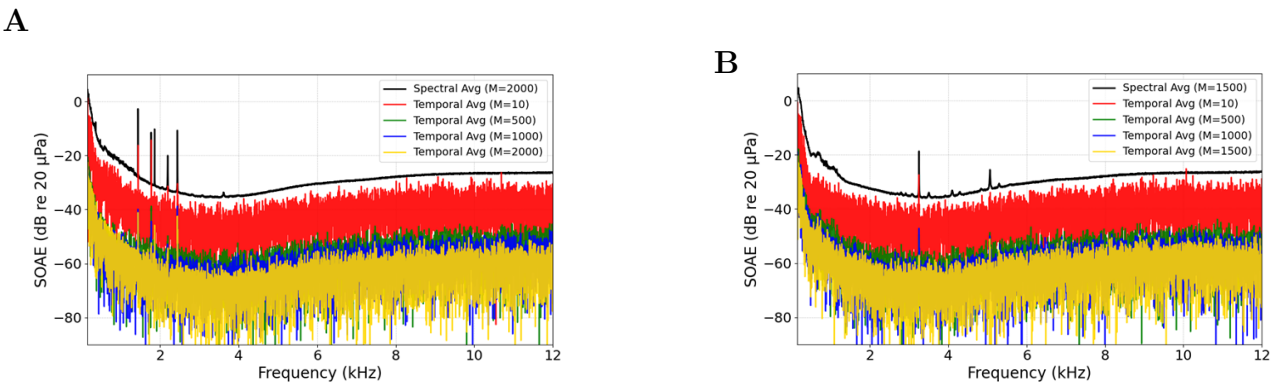

Figure A.6: Human 30-minutes time waveform. (A) Subject 1 (B) Subject 2.